Annales Societatis Geologorum Poloniae (2014), vol. 84: 185–212.

ORGANIC GEOCHEMICAL STUDY OF THE LOWER MIOCENE KREMNA BASIN, SERBIA

Tamara PERUNOVIĆ[1], Ksenija STOJANOVIĆ[1], Vladimir SIMIĆ[2], Milica KAŠANIN-GRUBIN[3], Aleksandra ŠAJNOVIĆ[3], Vladisav ERIĆ[4], Jan SCHWARZBAUER[5], Nebojša VASIĆ[2], Branimir JOVANČIĆEVIĆ[1] & Ilija BRČESKI[1]

[1] University of Belgrade, Faculty of Chemistry, Studentski trg 12-16, 11000 Belgrade, Serbia; e-mails: tamara.perunovic@gmail.com, ksenija@chem.bg.ac.rs, bjovanci@chem.bg.ac.rs, ibrceski@chem.bg.ac.rs
[2] University of Belgrade, Faculty of Mining and Geology, Djušina 7, 11000 Belgrade, Serbia; e-mails: simicv@rgf.bg.ac.rs, sedimentologija@yahoo.com
[3] University of Belgrade, Center of Chemistry, IChTM, Studentski trg 12-16, 11000 Belgrade, Serbia; e-mails: mkasaningrubin@chem.bg.ac.rs, sajnovica@chem.bg.ac.rs
[4] Rio Tinto – Rio Sava Exploration, Takovska 45, 11000 Belgrade, Serbia e-mail: vladisav.eric@riotinto.com
[5] RWTH Aachen University, Institute of Geology and Geochemistry of Petroleum and Coal, Lochnerstr. 4-20, 52056 Aachen, Germany; e-mail: jan.schwarzbauer@emr.rwth-aachen.de

Perunović, T., Stojanović, K., Simić, V., Kašanin-Grubin, M., Šajnović, A., Erić, V., Schwarzbauer, J., Vasić, N., Jovančićević, B. & Brčeski, I., 2014. Organic geochemical study of the Lower Miocene Kremna Basin, Serbia. *Annales Societatis Geologorum Poloniae*, 84: 185–212.

Abstract: The Kremna Basin is located in southwest Serbia, in the Zlatibor area, which is part of the Internal Dinarides. This basin is noteworthy because of the type of bedrock drainage, which it represents. It was formed on ultrabasic rocks and volcanic materials that influenced the occurrence of organic matter (OM) in the basin fill. The objective of the study was to determine the organic geochemical characteristics of sediments from the central part of the Kremna Basin.

The sediments studied belong to an intrabasinal facies, in which two sequences were distinguished. The lower sequence occurs at depths of 216–343 m, while the upper sequence is found from 13.5–216 m.

At the start of basin development (265–343 m) sedimentation took place in shallow alkaline water, rich in Mg ions. Through time, a slight deepening of the basin occurred. This was followed by chemical deposition of carbonates (216–265 m). The most important change in the sedimentary environment occurred with the formation of sediments marking the transition between the sequences (at about 200 m).

Sediments from the lower sequence are characterized by the dominance of dolomite and magnesite. There are indications of volcanic activity, i.e. tuff layers and the presence of searlesite. The upper sequence is characterized by the prevalence of calcite and dolomite. The amounts of MgO, Na_2O and B are higher in the lower sequence, whereas the CaO content is higher in the upper sequence.

The sediments contain different amounts of immature OM (late diagenesis). Biomarker analysis shows diverse precursors of the sedimentary OM: methanogenic archaea, photosynthetic green sulfur bacteria (*Chlorobiaceae*), bacterivorous ciliates, various bacteria, both photosynthetic and non-photosynthetic, the green unicellular microalga, *Botryococcus braunii* race A (exclusively in the upper sequence) and terrestrial plants. The lower sequence contains lower amount OM, composed primarily of kerogen II/III and III types, indicating a higher contribution of the allochtonous biomass of land plants from the lake catchment, particularly in the lower part. The sediments of the upper sequence are enriched in autochthonous aquatic OM, which comprises mostly kerogen I, I/II and II types. The transition from the lower sequence to the upper one is associated with a decrease in pristane to phytane ratio, gammacerane index and content of C_{28} steroids, absence or significantly lower amount of squalane, absence of C_{24} and C_{25} regular isoprenoids, 8-methyl-2-methyl-2-(4,8,12-trimethyltridecyl) chroman and C_{30} hop-17(21)-ene.

Pyrolytic experiments showed that the sediments of the upper sequence, rich in aquatic OM, at a catagenetic stage could be a source of liquid hydrocarbons. The values of hopane, sterane and phenanthrene maturation parameters indicate that through pyrolysis at 400°C the samples investigated reached a value of vitrinite reflectance equivalent of approximately 0.70%. It was estimated that the sediments should be found at depths of 2300–2900 m in order to become active source rocks. The calculated minimum temperature, necessary for catagenetic hydrocarbon generation, is between 103 and 107°C.

Key words: Kremna Basin, lacustrine sediments, organic matter, mineralogy, biomarkers, pyrolysis.

Manuscript received 6 December 2013, accepted 17 September 2014

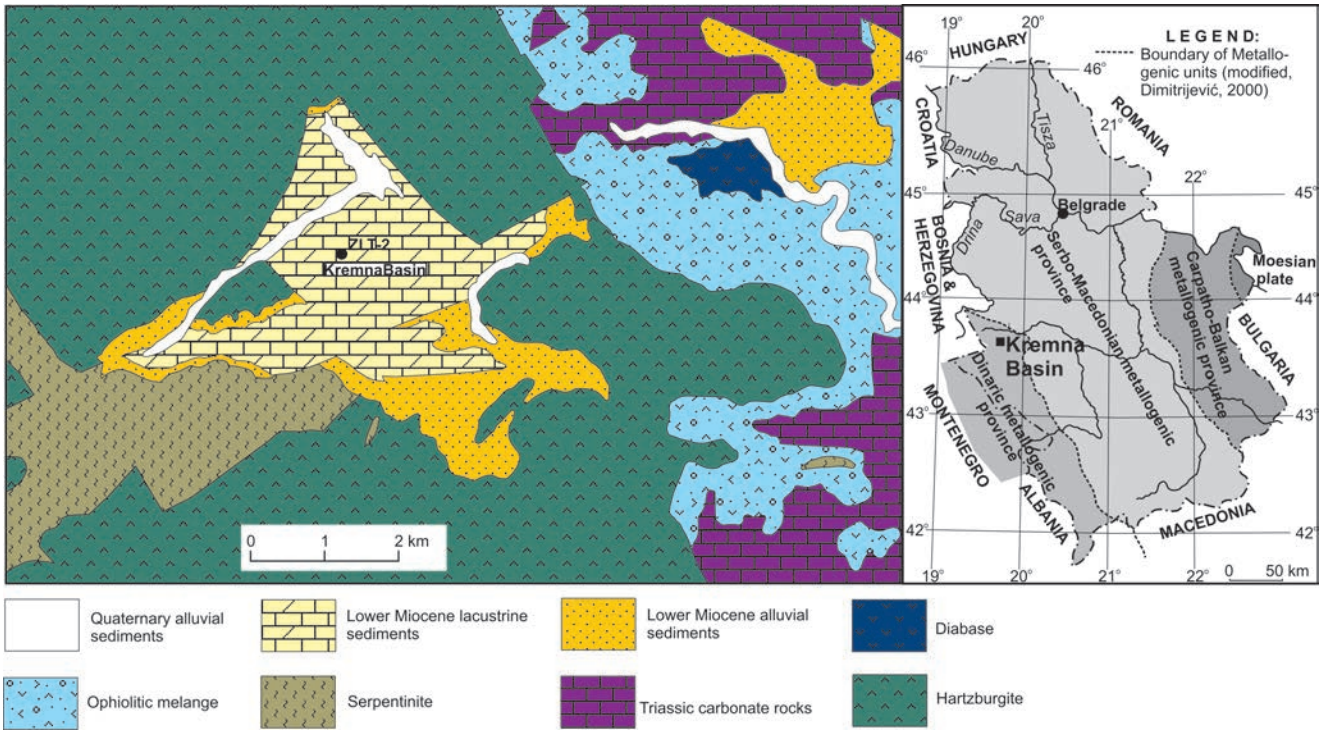

Fig. 1. Location and simplified geological map of Kremna Basin (modified after Basic Geologic Map of SFRJ, Užice Sheet, Mojsilović *et al*., 1973), showing location of sampled ZLT-2 borehole.

INTRODUCTION

Hydrology (water output and input of surface water, rainfall, and groundwater), sediment input, and temperature changes represent three major factors which control sedimentation patterns, and thus carbonate deposition in lake basins (Tucker and Wright, 1990; Platt and Wright, 1991). These factors are influenced by both climate and tectonics (Bohacs *et al*., 2000, 2003). Considering the complexity of sedimentation in lake basins, an understanding of the sedimentation history requires a variety of sedimentological, palaeontological and geochemical analyses.

Bioproductivity in lacustrine environments can be as high as ten times, than in marine environments. Under such conditions, preservation of the organic matter can be favoured as well (Peters *et al.*, 2005). These two factors contribute to formation of sediments rich in organic matter (OM).

Despite of the influence of oxidation processes, which favour the OM degradation, organic carbon content (Corg) is often used as a preliminary palaeoproductivty indicator (Meyers, 1997). Rock-Eval pyrolysis is used as a rapid, preliminary method for examining the origin/type and maturity of the organic matter (Espitalié *et al*., 1985).

The conditions of sedimentation determine the carbon to nitrogen ratio (C/N) in OM-rich sediments (Meyers, 1994; Mackie *et al*., 2005). The C/N ratio lower than 10 is typical for algal material, which is depleted in cellulose in comparison to OM originated from higher plants (Meyers and Ishiwatari, 1993). Values of C/N ratio over 20 can be considered an indicator of a greater contribution of higher terrestrial plant material as a precursor for the OM (Meyers, 1994). However, an elevated C/N ratio also may be a consequence of the easier degradation of algal OM, rich in labile nitrogen, during diagenesis (Meyers, 1994).

Analysis of the extractable organic matter (bitumen) taken from sediments has been proven to be a promising tool for reconstruction of the sedimentary environment as well as the precursor biomass and its transformation during diagenesis. The analysis of bitumen is based on identification of finger print compounds (biomarkers) which are by structure strongly related to precursor biomolecules from organisms. Numerous parameters for biomarkers are used in the assessment of the origin, depositional environment and maturity of the OM (Peters *et al*., 2005, and references therein). Apart from the analyses mentioned, a full characterisation of the OM in sedimentary rocks also requires the investigation of the kerogen. In the case of an immature sample, its potential might be estimated by simulation of changes in organic matter maturity under laboratory conditions, using different pyrolytic experiments (Huizinga *et al*., 1988; Yoshioka and Ishiwatari, 2002; Parsi *et al*., 2007; Budinova *et al*., 2014, and references therein).

The objective of the study was to determine the organic-geochemical characteristics of sediments from the central part of the Kremna Basin. This basin is noteworthy, because of the specific palaeorelief, type of bedrock drainage and volcanic input that influenced the development of organic matter. For this purpose, the major-element content, bulk and specific organic-geochemical parameters, and qualitative mineralogical composition were investigated. Pyrolytic experiments were performed on bitumen-free samples in a detailed study of the *l*iquid-hydrocarbon potential of the sediments for prediction of the conditions necessary for them to become active oil-generating source rocks.

GEOLOGICAL SETTING

The Zlatibor area is located in SW Serbia, about 200 km SW of Belgrade (Fig. 1). As a part of the Internal Dinarides, it consists mostly of a Dinaric ophiolite nappe, which was emplaced during the Jurrasic (Ilić and Neubauer, 2005). During the middle early Miocene, the Zlatibor area was affected by the opening of Dinaride Lake system (Krstić *et al*., 2001). The relics of Miocene sediments are preserved only locally (the Kremna, Bioska, Mačkat, Kačer and Braneš basins), usually fault-bounded and interbedded with fine-grained volcanic tuffs and rarely with coal.

According to recent palaeontological investigations, the age of the sedimentary units is early Miocene, between 19 and 17 Ma (Prysjazhnjuk *et al*., 2000; Krstić *et al*., 2001). The only known fossil flora remains in the Kremna Basin were interpreted as early Miocene (Pantić, 1956). A rare fossil fauna (*Planorbis*, *Unio*, *Bithinia*) and ostracoda also were found, indicating the same age (Eremija, 1977). The whole Dinarides subsequently were affected by late Neogene and Quaternary uplift and denudation (Marović *et al*., 1999, 2002).

Sedimentation in the Kačer and Bioska basins was dominated by clastic rocks, while in the Kremna Basin, carbonate rocks also were deposited in addition to clastics (Obradović and Vasić, 2007). This study is focused on the Kremna Basin, covering an area of approximately 15 km^2 (Fig. 1). The Kremna Basin was previously investigated for potential deposits of boron and magnesite as well as sepiolite and palygorskite clay (Živković and Stojanović, 1976; Dedić, 1978; Ilić and Rubežanin, 1978; Obradović *et al*., 1994, 1995; Kovačević, 1998).

The bedrock that underwent erosion during basin evolution consisted primarily of Jurassic ultrabasic rocks, serpentinite and ophiolitic mélange, and Triassic carbonate rocks (Fig. 1). Intense weathering of ultramafic rocks during the Palaeogene formed a thick weathering crust of smectite (Maksimović, 1996). The weathering processes yielded intense leaching of MgO, which consequently influenced the formation of magnesite rich sedimentary rocks.

Obradović and Vasić (2007) summarized previous studies of the Kremna Basin and on the basis of the results presented by Dedić (1978), they distinguished alluvial and lacustrine series, and in them marginal and intrabasinal facies. The alluvial series consists of conglomerates and sandstones made up of ultramafic rock fragments (Obradović and Vasić, 2007). Thin intercalations of coal (2–5 cm thick) are found in these sediments (Dedić, 1978). Marginal lacustrine and intrabasinal lacustrine facies consist of carbonate sediments, namely dolomite and/or magnesite, marlstones and rarely limestone (Obradović *et al*., 1996).

MATERIALS

For the purpose of this study, 43 core samples (5–10 cm in length) were taken from the ZLT-2 borehole at different depths. Sample preparation for chemical analyses was performed at the Institute for Technology of Nuclear and Mineral Raw Materials (ITNMS), Belgrade. The sediment samples were dried at 105°C. In the next step, the samples were successively crushed to 2.36 mm in three stages, using a jaw crusher, a cone crusher and a roller crusher, respectively. Then the samples were homogenized. A rough mill-fragmented sample was subsequently finely pulverized and sifted through a 63 μm sieve. Whole rock samples for thin sections and scanning electron microscopy (SEM) analyses were taken separately from the core.

METHODS

X-Ray diffraction analysis

X-ray diffraction analyses were performed in the Laboratory for Crystallography, Faculty of Mining and Geology, University of Belgrade, Serbia. For determination of the qualitative composition of the minerals, an X-ray generator PHILIPS Type PW 1729, and a diffractometer from the same manufacturer, type PW 1710 with genuine software processing (Philips APD), were used. As a source of radiation, an X-ray LLF-type tube with a copper anticathode and arched graphite monochromator placed between the sample and the detector were used, so that the radiation was CuK_{a1} = 1.5405 Å, thus avoiding possible X-ray fluorescence. The anode tube load was 40 kV and 35 mA. The gaps (slits) were fixed at 1.0 and 0.1 mm. Samples were pressed into standard aluminum frames and recorded in the range of 2Θ from 5° to 60°. Data were collected by measuring each of 1/50° (0.02°) for a duration of 0.5 sec. Identification of minerals was performed by comparing d_{hlk} values with those of the standards from an electronic database (Joint Committee on Powder Diffraction Standards, JCPDS-International Centre for Diffraction Data).

Determination of contents of major and trace elements

The contents of major and trace elements were determined at AcmeLabs, in Canada. Prepared samples were mixed with an $LiBO_2/Li_2B_4O_7$ flux. The crucibles were fused in a furnace. The cooled bead was dissolved in ACS-grade nitric acid. The amounts of Al_2O_3, CaO, Cr_2O_3, Fe_2O_3, K_2O, MgO, MnO, Na_2O, P_2O_5, SiO_2 and TiO_2 were determined by inductively coupled plasma-optical emission spectroscopy (ICP-OES). The amounts of Ba, Co, Cs, Rb, Sb, Sr, Th, U, V, Y and Zr were determined by inductively coupled plasma mass spectrometry (ICP-MS). The ICP-OES analysis was performed, using a SPECTRO ARCOS instrument, while for ICP-MS analysis an ELAN 9000 from Perkin Elmer was employed. A rack of 40 samples on either instrument comprised 36 samples, one analytical blank, one sample replicate, one internal reference material (IRM) and one of the Certified Reference Materials (CRM). Loss on ignition (LOI) was determined by igniting a sample split, then measuring the weight loss. Additionally, for the screening of possible occurrences of B and Li, the amounts of these two elements, together with the percentages of major elements and Sr (due to correlation) in core samples at 10 m intervals, were also determined. These analyses were performed in the Société Générale de Surveillance (SGS) Laboratory, Canada, following procedures that were described in previous papers (Šajnović *et al*., 2009, 2012).

Scanning electron microscopy (SEM)

SEM analyses were performed on gold-coated, polished thin sections at the Faculty of Mining and Geology, University of Belgrade, Serbia. Scanning electron microscopy was used for imaging and collecting chemical data, using a JEOL JSM–6610 LV Scanning Electron Microscope, equipped with an energy-dispersive spectrometer (EDS). Analyses were run at an accelerating voltage of 20 kV, and a working distance of 10 mm.

Rock Eval pyrolysis

Rock-Eval pyrolysis was performed at the Institute of Geology and Geochemistry of Petroleum and Coal, Aachen University, Germany. Depending on mineral composition, the amounts of macro-elements, the organic carbon content and the biomarker composition, twenty-five samples were selected for Rock-Eval pyrolysis. Measurements were carried out, using a DELSI INC Rock-Eval VI instrument, according to guidelines published by Espitalié *et al*. (1985) and Lafargue *et al*. (1998). About 100 mg of each powdered sample were pyrolyzed.

Determination of organic carbon, sulphur and nitrogen contents and bitumen analysis

Analyses were performed at the Faculty of Chemistry, University of Belgrade, Serbia. Elemental analysis was applied to determine the amounts of carbon, sulphur and nitrogen. Organic carbon (Corg) was determined after the removal of carbonates with diluted hydrochloric acid (1:3 v/v). The measurements were performed, using a Vario EL III, CHNOS Elemental Analyser, Elementar Analysensysteme GmbH (CHNS operation mode: furnace temperature 1150°C with a thermoconductivity detector, TCD).

Extractable organic matter (bitumen) was removed from the sediments by Soxhlet's extraction with an azeotrope mixture of dichloromethane and methanol (88:12 volume %), for 42 h (Šajnović *et al.*, 2009, 2012). Separation of the bitumen into the saturated and aromatic hydrocarbon fractions was achieved, using column chromatography (adsorbents: SiO_2, 2.88 g and Al_2O_3, 2.12 g; eluents, including a "dead volume" of 1.2 cm^3: *n*-hexane, 50 cm^3 and benzene, 25 cm^3; per 10 mg of bitumen).

The saturated and aromatic fractions, isolated from the initial bitumen and liquid pyrolysates, were analyzed by means of the gas chromatography-mass spectrometry (GC- MS) techique. The GC-MS was performed using an Agilent 7890A gas chromatograph (HP-5MS column, 30 m × 0.25 mm, 0.25 μm film thickness, He carrier gas 1.5 cm^3/min), coupled to an Agilent 5975C mass selective detector (70 eV). The column was heated from 80 to 310°C, at a rate of 2°C/min., and the final temperature of 310°C was maintained for an additional 25 minutes. The individual peaks were identified on the basis of comparison of the mass spectrum obtained with those from the literature (Risatti *et al*., 1984; Philp, 1985; Radke, 1987; Sinninghe Damsté *et al*., 1987; Koopmans *et al*., 1996a; Peters *et al.*, 2005) and the mass spectra library (NIST5a). Quantification of amounts of the compounds for calculating the molecular parameters was performed by integration of peak areas (software GCMS Data Analysis) in the appropriate mass chromatograms [*m/z* 71 for *n*-alkanes; *m/z* 217 for steranes; *m/z* 215 for sterenes; *m/z* for 191 hopanes and *m/z* 121, 135 and 149 for mono-, di- and trimethylated 2-methyl-2-(4,8,12-trimethyltridecyl) chromans, respectively]. Methyl-, dimethyl- and trimethylnaphthalenes in the aromatic fractions of liquid pyrolysates were identified from the *m/z* 142, 156, and 170 ion fragmentograms, whereas phenanthrene, methyl-, and dimethylphenanthrene isomers were analyzed from the *m/z* 178, 192, and 206 ion fragmentograms.

Pyrolysis of the samples rich in organic matter

Pyrolysis was performed on samples free of soluble organic matter (bitumen), which contained kerogen with a native mineral matrix. The initial mass of a bitumen-free sample was ~5 g. Pyrolyses were performed in an autoclave under nitrogen for 4 hours at 400°C. Liquid pyrolysis products were extracted with hot chloroform. The gaseous products were not analyzed, although the production of gaseous products was indicated by the pressure change in the autoclave. Liquid pyrolysates were separated into saturated hydrocarbon, aromatic hydrocarbon, and NSO fractions using the same method as applied in the fractionation of extracted bitumen. The saturated and aromatic fractions were analyzed by GC-MS, as described in the previous section.

RESULTS

Mineral composition and content of major elements

The chemical composition of the sediments from the Kremna Basin was determined for 43 core samples (Tables 1–3). Samples for mineralogical and petrological analyses (thin section and SEM) were selected with reference to the analyses obtained.

Generally, the mineral composition of the Kremna Basin sediments is represented by dolomite, quartz, calcite, magnesite, and clay minerals. Different lacustrine facies could not be clearly distinguished from the results obtained. However, it was evident that the sediments from the core analyzed belong to an intrabasinal facies (Figs 2, 3).

Sediments from the lower sequence in the core (216–343 m) contain more Mg-rich minerals (Fig. 3B) and the Mg originated from the underlying ultramafites. This section is characterised by pronounced volcanic activity (tuff, searlesite; Fig. 3C). The spherulitic structure, common in silica-rich glassy rocks, is visible in thin (20–30 cm) potassium-rich unaltered volcanic material (depth 262 m; Figs 2, 4A, B). The glass is occasionally devitrified and the spherulites are recrystallised. Clay minerals are poorly represented in the entire column, except in intervals where sepiolite and smectite occur by paragenesis with dolomite and magnesite (Fig. 3D). Ca-rich sediments are dominant in the upper sequence of the core (13.5–216 m, Fig. 3A). Volcanic material was also determined in a thin layer at a depth of 77.5 m (Figs 2, 4C, D).

Table 1

Amounts of major elements (weight %) in sediments

Sequence	Description	No	Depth (m)	SiO_2	Al_2O_3	Fe_2O_3	MgO	CaO	Na_2O	K_2O	TiO_2	P_2O_5	MnO	Cr_2O_3	LOI*
Clayey carbonates		1	11.5	55.57	0.94	1.03	4.97	8.88	0.12	0.47	0.04	0.01	0.01	0.02	28.6
Upper sequence (US)	Marly dolomite	2	13.5	8.40	1.02	0.81	16.19	22.19	0.09	0.56	0.03	0.01	0.02	0.02	50.7
		3	27	17.44	3.03	1.31	14.46	21.58	0.11	1.42	0.07	0.02	0.03	0.02	40.5
		4	32	12.62	1.87	0.69	19.4	22.43	0.11	1.13	0.04	0.01	0.02	0.01	41.8
		5	42.5	15.02	3.04	1.44	2.15	37.64	0.07	1.51	0.06	0.02	0.05	0.01	39.4
		6	54	34.79	6.80	2.33	11.15	9.24	0.08	2.63	0.12	0.01	0.03	0.02	34.3
		7	55.5	26.09	1.97	0.81	15.63	18.86	0.08	0.67	0.04	0.03	0.03	0.01	36.6
		8	64.5	17.58	0.61	0.21	17.1	23.15	0.08	0.18	0.01	0.01	0.01	0	41
	Marlstone, calcite dominated	9	70	30.34	6.04	1.80	2.27	27.7	0.06	1.47	0.09	0.01	0.04	0.02	31.7
		10	78	10.24	2.09	0.69	11.21	32.77	0.13	0.47	0.04	0.01	0.02	0	42.5
		11	80	10.68	2.38	0.53	6.08	36.77	0.11	0.36	0.05	0.02	0.02	0	43.6
		12	83	11.99	3.31	0.88	2.43	41.81	0.15	0.41	0.07	0.04	0.02	0.01	39.9
		13	96	10.98	3.18	1.44	1.50	42.84	0.13	0.55	0.08	0.11	0.03	0.01	39.9
		14	111	12.45	2.59	0.80	2.52	36.33	0.14	0.53	0.05	0.15	0.02	0.01	45
		15	113	22.39	5.46	2.68	1.47	35.35	0.20	1.19	0.28	0.04	0.06	0.04	31.9
		16	127	18.28	5.18	2.57	1.69	38.01	0.25	1.12	0.14	0.04	0.04	0.03	33.6
		17	137.5	6.98	1.18	0.63	2.66	44.58	0.15	0.24	0.03	0.06	0.01	0.01	43.6
		18	150	27.69	1.87	0.87	1.09	32.43	0.16	0.39	0.13	0.01	0.02	0.02	36.6
		19	164	13.99	1.82	1.16	1.21	43.88	0.20	0.41	0.07	0.12	0.03	0.02	37.7
		20	185	17.16	1.04	0.76	7.51	29.38	0.23	0.36	0.03	0.07	0.02	0.01	43.8
		21	189.5	23	1.39	1.20	8.88	26.89	0.22	0.71	0.04	0.05	0.03	0.02	37.7
Lower sequence (LS)	Marly laminated magnesite	22	216	36.81	0.31	0.96	21.41	13.46	0.41	0.10	0.02	0.01	0.01	0.02	28.3
		23	219	12.91	0.85	1.24	35.35	5.99	0.29	0.29	0.02	0.01	0.02	0.03	42.8
		24	224	24.05	1.79	2.51	20.39	17.10	0.45	0.80	0.06	0.01	0.05	0.05	33.8
		25	238	46.93	4.89	1.17	24.44	2.36	1.24	2.79	0.03	0.01	0.02	0.01	20.4
		26	243.5	16.61	0.94	1.19	32.75	6.29	1.19	0.48	0.04	0.01	0.02	0.02	40.6
		27	245	16.44	0.73	2.66	35.98	4.79	0.69	0.27	0.03	0.01	0.04	0.08	39.1
		28	248.3	19.39	0.66	1.34	30.28	6.50	2.28	0.29	0.03	0.01	0.02	0.03	39.4
		29	255	12.26	0.60	1.20	36.68	4.58	0.70	0.22	0.03	0.01	0.03	0.05	43.8
		30	258	40.14	3.40	8.85	20.92	6.15	1.71	1.60	0.11	0.01	0.11	0.19	21
		31	265	15.93	1.30	1.95	33.62	5.84	1.40	0.62	0.05	0.01	0.03	0.03	39.9
	Marly Mg dolomite, Silty Mg-marlstone, Mg-clay	32	283	20.75	1.35	1.89	26.3	13.79	1.16	0.45	0.05	0.01	0.03	0.04	35.7
		33	286	29.18	2.27	3.46	24.87	11.49	1.56	0.66	0.08	0.02	0.04	0.06	29
		34	297.5	23.76	2.09	1.92	28.62	9.19	1.53	0.44	0.07	0.01	0.03	0.03	34.3
		35	309	33.83	4.62	5.93	21.84	9.25	2.23	1.23	0.19	0.02	0.07	0.08	24.1
		36	317.5	22.68	2.19	2.72	25.39	12.59	1.45	0.53	0.08	0.01	0.04	0.05	33.7
		37	324	34.6	3.65	5.08	23.11	7.70	1.98	1.07	0.12	0.02	0.06	0.1	25.7
		38	329	34.22	4.05	5.51	19.05	10.76	1.83	1.61	0.13	0.02	0.06	0.11	25.6
		39	335	27.27	0.06	0.15	23.9	13.48	2.11	0.07	0.01	0.02	0.07	0.01	35.8
		40	336	23.11	0.28	0.19	22.58	14.3	2.10	0.07	0.01	0.02	0.04	0.01	39.6
		41	340	43.08	1.51	5.53	22.88	2.96	1.9	0.34	0.04	0.02	0.03	0.1	27.2
		42	341	46.15	2.37	8.17	20.53	2.93	2.22	0.53	0.07	0.02	0.04	0.15	22.8
		43	343	52.4	4.39	11.55	16.66	0.68	2.12	2.39	0.12	0.02	0.03	0.2	15.6
Minimum US				6.98	0.61	0.21	1.09	9.24	0.06	0.18	0.01	0.01	0.01	0	31.7
Maximum US				34.79	6.8	2.68	19.4	44.58	0.25	2.63	0.28	0.15	0.06	0.04	50.7
Average US				17.41	2.79	1.18	7.33	31.19	0.14	0.82	0.07	0.04	0.03	0.01	39.59
Standard deviation US				7.71	1.77	0.69	6.37	9.57	0.06	0.6	0.06	0.04	0.01	0.01	4.75
Minimum LS				12.26	0.06	0.15	16.66	0.68	0.29	0.07	0.01	0.01	0.02	0.01	15.6
Maximum LS				52.4	4.89	11.55	36.68	17.1	2.28	2.79	0.19	0.02	0.11	0.2	43.8
Average LS				28.75	2.01	3.42	25.8	8.28	1.48	0.77	0.06	0.01	0.04	0.07	31.74
Standard deviation LS				11.83	1.52	3.05	5.89	4.55	0.64	0.74	0.05	0.01	0.02	0.06	8.14

* – Loss on ignition.

Table 2

Amounts of trace elements (mg/kg) in sediments

Sequence	Description	No	Depth (m)	Ba	Co	Cs	Rb	Sc	Sr	Th	U	V	Zr
Clayey carbonates		1	11.5	109.2	8.90	1.11	12.74	2.02	190.7	0.71	0.61	13.14	12.84
Upper sequence (US)	Marly dolomite	2	13.5	108.89	12.10	2.42	19.66	2.02	906.53	0.50	1.11	34.28	6.15
		3	27	451.39	10.88	11.79	70.33	3.02	815.82	1.41	0.81	20.15	24.08
		4	32	233.55	5.26	2.63	29.22	2.02	1227.88	1.72	0.81	12.13	6.77
		5	42.5	171.73	8.79	6.26	60.31	3.03	875.04	2.42	1.21	18.18	19.6
		6	54	201.46	14.49	10.79	116.76	4.11	984.89	2.06	0.51	39.06	31.86
		7	55.5	153.83	5.91	4.28	35.35	2.04	773.63	2.55	2.24	16.30	10.59
		8	64.5	93.51	1.21	1.41	9.85	0.50	794.57	0.40	0.80	8.04	9.15
	Marlstone, calcite dominated	9	70	307.76	10.57	16.82	82.17	4.10	1521.65	3.49	1.85	18.47	36.32
		10	78	515.36	3.44	7.68	25.97	2.02	1232.52	3.13	3.13	10.11	23.65
		11	80	388.01	2.23	6.09	24.58	1.02	926.26	1.93	2.03	14.22	32.61
		12	83	277.61	3.78	13.47	33.68	2.04	1404.16	2.55	1.33	15.31	14.9
		13	96	437.44	10.27	19.43	37.13	3.05	1291.05	2.75	1.73	19.33	14.34
		14	111	258.83	6.60	13.20	32.07	2.03	1144.74	2.33	2.84	16.24	14.41
		15	113	415.01	19.58	32.83	79.74	7.14	1258.59	7.85	3.26	61.18	35.28
		16	127	371.24	20.40	47.42	78.53	6.12	1707.29	3.47	1.84	41.82	27.03
		17	137.5	226.72	5.95	16.22	16.02	1.01	1193.97	0.91	1.11	12.09	7.76
		18	150	263.97	11.56	3.17	20.46	2.05	701.04	1.64	0.61	18.42	19.85
		19	164	247.16	11.75	1.72	19.65	3.04	944.89	1.72	1.32	17.22	16.00
		20	185	171.79	8.08	2.83	16.98	1.01	659.36	1.52	2.22	17.18	8.19
		21	189.5	149.99	11.88	2.92	31.11	2.01	600.56	1.31	1.51	17.11	10.57
Lower sequence (LS)	Marly laminated magnesite	22	216	82.59	10.94	0.31	4.96	1.03	1316.13	0.10	0.31	8.26	5.27
		23	219	134.59	15.69	0.81	12.85	2.02	2197.53	0.30	0.40	9.11	5.67
		24	224	338.81	29.88	1.44	26.49	4.11	2510.78	1.33	0.92	21.56	13.96
		25	238	108.22	7.75	0.53	19.31	1.06	861.64	0.74	0.42	4.24	21.96
		26	243.5	121.83	15.63	1.02	12.79	2.03	1484.67	0.51	0.51	12.18	8.32
		27	245	69.89	32.99	0.82	10.69	3.08	1276.57	0.21	0.41	18.50	5.45
		28	248.3	117.96	20.24	1.12	11.80	2.03	1869.33	0.20	0.61	10.17	4.47
		29	255	105.73	16.98	0.92	9.86	1.02	1514.95	0.31	0.41	11.18	4.27
		30	258	110.46	95.17	5.10	50.03	8.50	720.34	0.64	0.64	33.99	21.77
		31	265	82.85	21.79	2.56	17.80	2.05	1147.90	0.31	0.51	11.25	9.41
	Marly Mg-dolomite, Silty Mg-marlstone, Mg-clay	32	283	176.39	18.99	10.69	18.16	3.11	2992.01	0.83	0.83	14.53	10.27
		33	286	153.10	29.78	21.29	29.05	4.19	2209.94	0.84	0.63	20.97	18.67
		34	297.5	131.09	13.42	24.24	19.77	2.08	1557.95	0.94	0.31	16.65	29.44
		35	309	174.03	47.89	60.01	48.94	6.33	2301.13	1.48	0.53	30.59	37.23
		36	317.5	228.64	25.35	34.35	25.97	4.14	3252.12	0.83	0.52	21.73	15.62
		37	324	89.44	54.92	93.43	61.66	5.26	1174.56	0.74	0.42	35.77	24.31
		38	329	92.25	59.44	94.24	51.58	7.34	1244.16	0.73	0.73	38.79	24.74
		39	335	183.54	4.43	0.95	1.16	0.53	1187.45	0.84	0.53	4.22	14.56
		40	336	183.02	2.20	0.42	0.73	0.52	1063.38	1.36	1.57	4.18	8.47
		41	340	39.02	40.33	4.44	8.02	5.42	123.58	0.87	0.43	76.96	9.11
		42	341	32.58	54.73	5.54	11.84	8.69	105.12	1.41	0.43	83.61	12.16
		43	343	17.29	64.4	12.75	52.62	11.89	24.53	1.19	0.22	106.97	19.45
Minimum US				93.51	1.21	1.41	9.85	0.50	600.56	0.40	0.51	8.04	6.15
Maximum US				515.36	20.40	47.42	116.76	7.14	1707.29	7.85	3.26	61.18	36.32
Average US				272.26	9.24	11.17	41.98	2.67	1048.22	2.28	1.61	21.34	18.46
Standard deviation US				121.53	5.21	11.62	29.00	1.67	301.81	1.57	0.81	12.95	9.97
Minimum LS				17.29	2.20	0.31	0.73	0.52	24.53	0.10	0.22	4.18	4.27
Maximum LS				338.81	95.17	94.24	61.66	11.89	3252.12	1.48	1.57	106.97	37.23
Average LS				126.06	31.04	17.13	23.00	3.93	1460.72	0.76	0.56	27.06	14.75
Standard deviation LS				71.25	23.29	28.74	18.29	3.05	866.2	0.42	0.28	27.63	8.98

Table 3

Amounts of major (weight %) and trace elements B, Li, Sr (mg/kg) in core samples at 10-m intervals

Sequence	Description	Depth (m)	SiO_2	Al_2O_3	Fe_2O_3	MgO	CaO	Na_2O	K_2O	TiO_2	P_2O_5	MnO	Cr_2O_3	B	Li	Sr
Upper sequence (US)	Marly dolomite	10-20	12.10	0.62	0.60	18.40	25.50	0.16	0.24	0.02	0.01	0.02	0.02	95	290	1200
		20-30	9.61	1.60	1.05	9.19	34.50	0.10	0.73	0.05	0.01	0.03	0.03	87	84	1300
		30-40	22.20	2.47	1.14	17.80	18.80	0.16	1.47	0.04	0.01	0.03	0.01	73	460	1200
		40-50	12.80	1.64	0.97	11.90	30.80	0.11	0.75	0.04	0.02	0.04	0.02	140	130	1000
		50-60	18.00	2.37	0.94	12.50	25.80	0.12	1.11	0.05	0.01	0.03	0.03	96	210	860
		60-70	14.30	2.21	0.98	7.48	33.00	0.12	0.63	0.05	0.01	0.05	0.02	110	110	1300
	Marlstone, calcite dominated	70-80	24.40	2.11	0.60	10.40	25.10	0.12	1.18	0.03	0.01	0.02	0.03	71	81	740
		80-90	7.82	1.46	0.46	2.97	43.40	0.25	0.24	0.03	0.05	0.03	0.01	69	34	1700
		90-100	8.64	0.83	1.03	13.60	32.10	0.32	0.25	0.03	0.04	0.03	0.02	280	85	1400
		100-110	5.74	0.91	0.44	2.68	45.80	0.20	0.18	0.03	0.12	0.02	0.01	100	20	1600
		110-120	19.00	3.10	1.05	3.75	34.30	0.19	0.61	0.07	0.08	0.03	0.02	81	27	1400
		120-130	9.15	1.54	0.94	4.13	40.40	0.25	0.37	0.04	0.11	0.03	0.01	62	20	1300
		130-140	10.00	0.99	0.78	5.40	39.00	0.14	0.23	0.03	0.08	0.04	0.02	57	20	1200
		140-150	12.40	1.55	0.96	2.57	41.10	0.23	0.35	0.05	0.08	0.04	0.02	72	20	1400
		150-160	12.20	1.79	0.96	6.71	35.80	0.19	0.41	0.05	0.05	0.04	0.02	39	20	580
		160-170	14.00	1.35	0.86	6.94	35.00	0.17	0.32	0.04	0.06	0.04	0.01	52	21	610
		170-180	13.50	1.67	0.94	6.41	35.90	0.35	0.46	0.04	0.04	0.02	0.02	76	33	630
		180-190	16.70	1.84	1.24	7.68	32.30	0.27	0.54	0.06	0.03	0.04	0.03	76	50	620
		190-200	44.90	7.33	1.63	4.42	14.00	1.78	1.90	0.12	0.05	0.06	0.03	77	20	320
		200-210	12.60	1.47	1.42	7.38	36.30	0.19	0.57	0.06	0.01	0.04	0.03	74	62	670
Lower sequence (LS)	Marly laminated magnesite	210-220	21.70	1.92	1.64	20.80	14.80	2.04	0.71	0.07	0.01	0.03	0.02	4400	390	3300
		220-230	13.40	0.78	1.22	34.10	6.95	0.31	0.30	0.03	0.01	0.03	0.04	300	190	1500
		230-235	13.10	1.02	1.23	33.30	7.22	0.36	0.44	0.03	0.01	0.03	0.03	190	170	1300
		235-240	12.10	0.66	0.75	36.30	5.58	0.35	0.24	0.02	0.01	0.02	0.03	320	140	1600
		240-245	14.50	0.93	2.08	32.80	6.31	0.52	0.39	0.03	0.01	0.03	0.05	680	160	1300
		245-250	14.90	0.88	1.89	29.90	8.90	0.99	0.41	0.04	0.01	0.03	0.05	2100	130	1200
		250-255	13.60	0.91	1.33	31.60	8.50	0.82	0.36	0.04	0.01	0.03	0.04	1600	110	1200
		255-260	16.70	1.28	1.64	29.10	8.39	1.39	0.59	0.04	0.01	0.04	0.04	2900	130	1300
		260-265	18.30	1.96	1.64	26.80	9.22	1.48	1.15	0.06	0.01	0.04	0.04	3700	140	1100
	Marly Mg-dolomite, Silty Mg-marlstone, Mg-clay	265-271	10.80	0.75	0.90	28.70	12.70	1.10	0.37	0.03	0.01	0.03	0.03	2600	150	2300
		271-281	15.00	0.86	1.08	24.70	16.60	0.99	0.32	0.04	0.02	0.03	0.02	1600	170	3400
		281-291	18.70	1.13	1.57	25.20	14.50	1.02	0.34	0.05	0.01	0.03	0.03	1300	270	2500
		291-301	18.70	1.34	1.40	26.70	12.30	1.15	0.32	0.06	0.01	0.03	0.03	1000	440	1900
		301-311	12.50	0.88	1.15	23.20	18.80	0.17	0.37	0.03	0.02	0.03	0.03	140	120	1200
		311-321	16.80	1.20	1.49	23.50	17.00	0.99	0.31	0.04	0.01	0.04	0.04	810	400	4200
		321-331	16.30	0.90	1.17	22.60	18.10	1.04	0.31	0.03	0.01	0.03	0.03	1400	420	2500
		331-342	19.60	0.90	2.17	31.40	5.62	0.97	0.31	0.03	0.01	0.03	0.05	830	220	480
Minimum US			5.74	0.62	0.44	2.57	14.00	0.10	0.18	0.02	0.01	0.02	0.01	39	20	320
Maximum US			44.90	7.33	1.63	18.40	39.00	1.78	1.90	0.12	0.12	0.06	0.03	280	460	1700
Average US			15.00	1.94	0.95	8.12	30.25	0.27	0.63	0.05	0.04	0.03	0.02	89	90	1052
Standard deviation US			8.48	1.40	0.29	4.70	7.96	0.36	0.46	0.02	0.04	0.01	0.01	50	112	393
Minimum LS			10.80	0.66	0.75	20.80	5.58	0.17	0.24	0.02	0.01	0.02	0.02	140	110	480
Maximum LS			21.70	1.96	2.17	36.30	18.80	2.04	1.15	0.07	0.02	0.04	0.05	4400	440	4200
Average LS			15.69	1.08	1.43	28.28	11.26	0.92	0.43	0.04	0.01	0.03	0.04	1522	221	1899
Standard deviation LS			3.01	0.37	0.39	4.55	4.61	0.48	0.22	0.01	0.00	0.00	0.01	1252	117	995

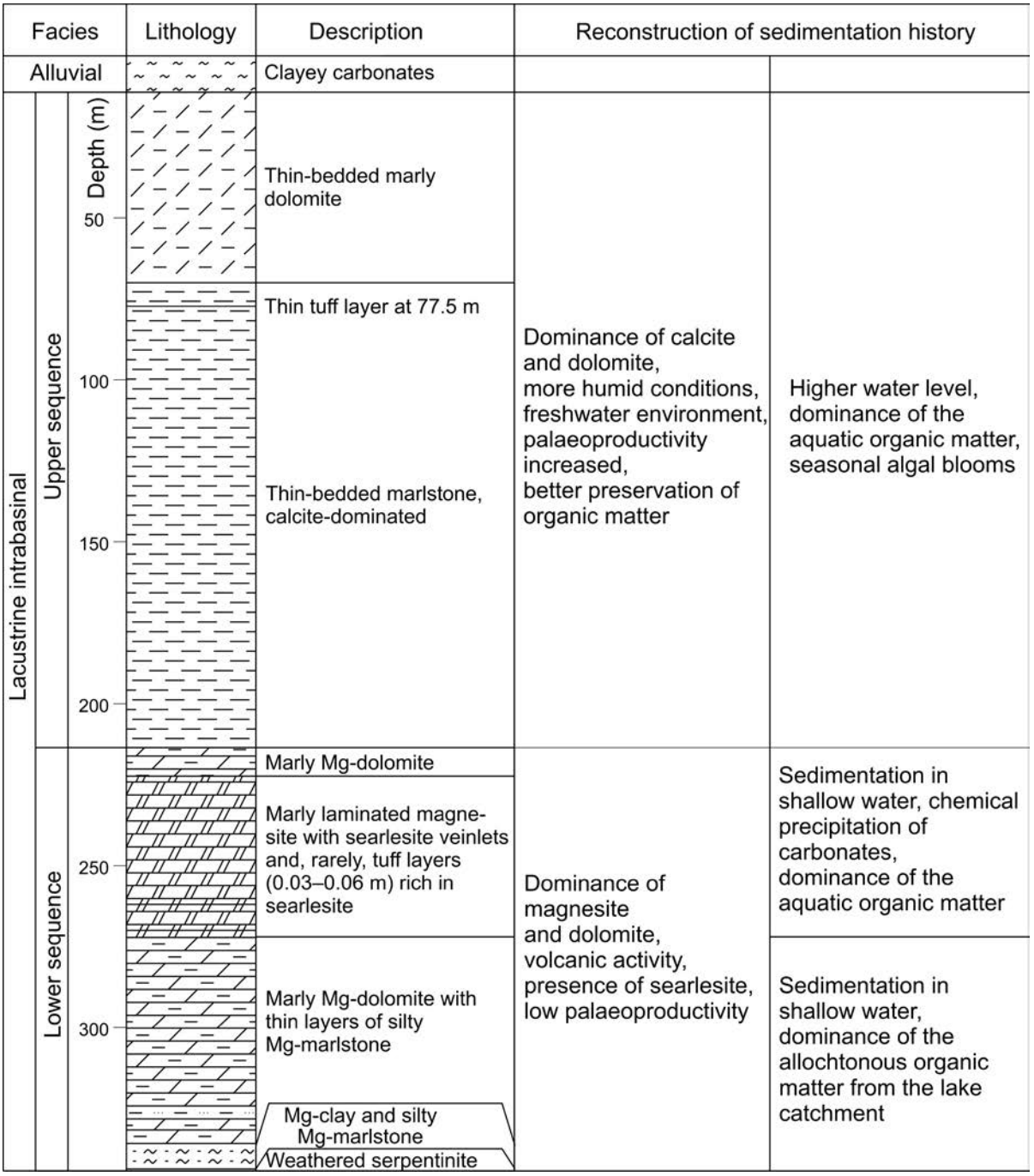

Fig. 2. Lithological column of ZLT-2 borehole.

The mineral content of the sediments from the Kremna Basin is reflected in their chemical composition. The lower sequence (216–343 m) has higher MgO, Na_2O, Fe_2O_3, SiO_2, B and Li contents, while the upper sequence (13.5–216 m) has a higher CaO content (Tables 1, 3). The entire core has a very low Al_2O_3 content (0.06–6.80%; Table 1), owing to the low clay content and a specific clay mineralogy with Mg clays predominant.

Bulk organic geochemical parameters and Rock Eval data

The OM content, expressed as total organic carbon (Corg), varies across a wide range of 0.32 to 12.38% (Table 4). The same observation is applicable to the amounts of extrac- table organic matter (bitumen) and both free (S1) and pyrolysis-derived bound hydrocarbons (S2), obtained by Rock-Eval pyrolysis (Tables 4, 5). Samples from the upper sequence are characterised by enhanced Corg, S1, S2 and nitrogen contents (Tables 4, 5). These results indicate that variations

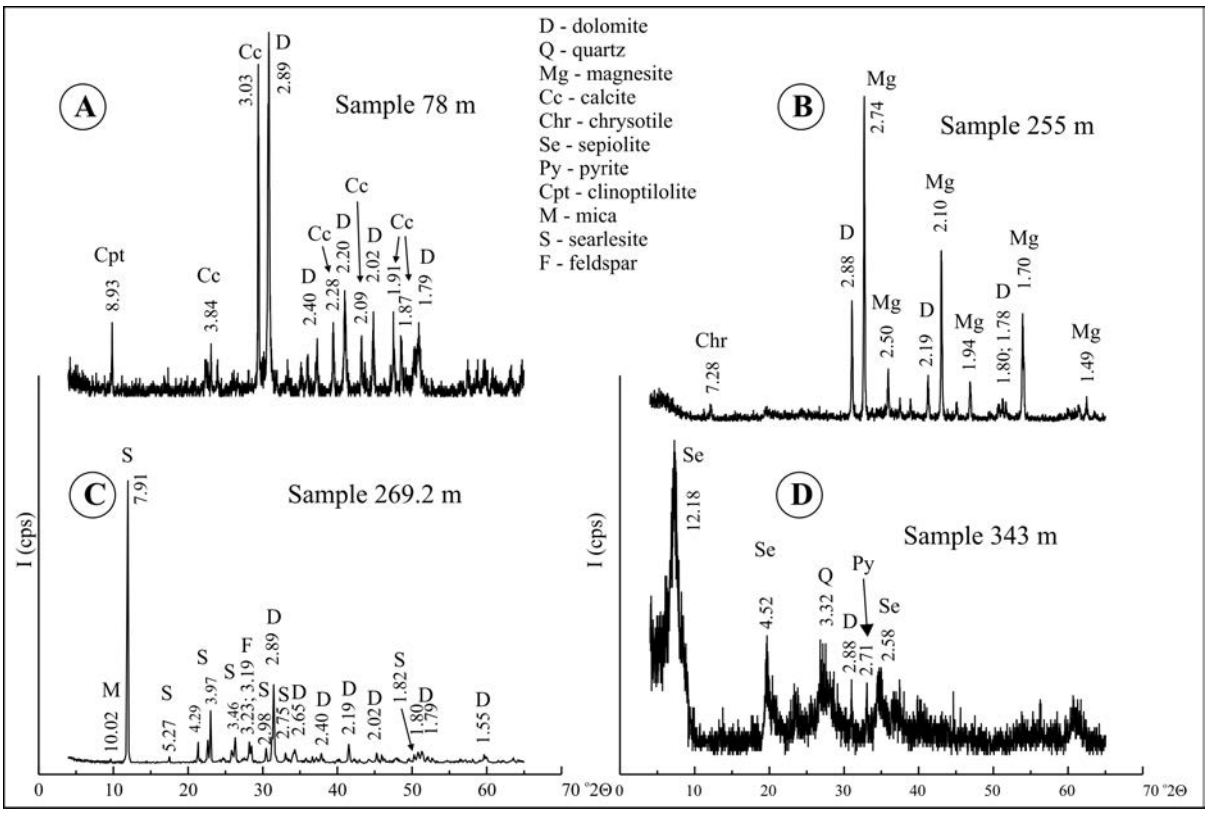

Fig. 3. Characteristic X-ray diffractograms of sediments from the Kremna Basin.

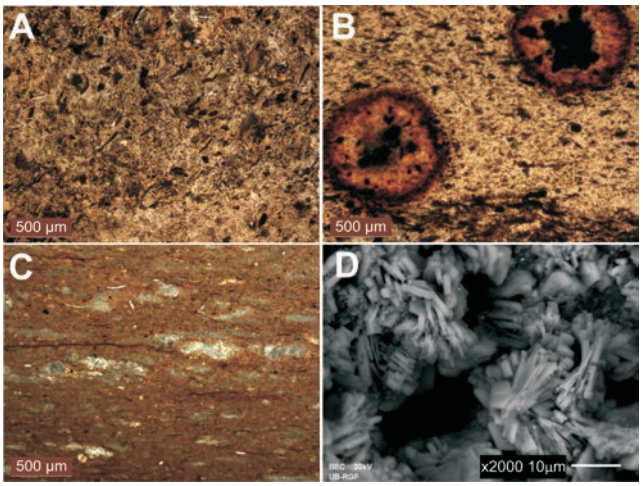

Fig. 4. Petrographic analyses of volcanic material from the Kremna Basin: (**A**) thin-section image of volcanic material containing biotite and glass, 262 m; (**B**) thin-section image of the same sample as under (A) showing sulphide minerals as centers of spherulites; (**C**) thin-section image of volcanic material with lamination and silica minerals in lenses, 77.5 m; (**D**) SEM image of the same sample as under (C).

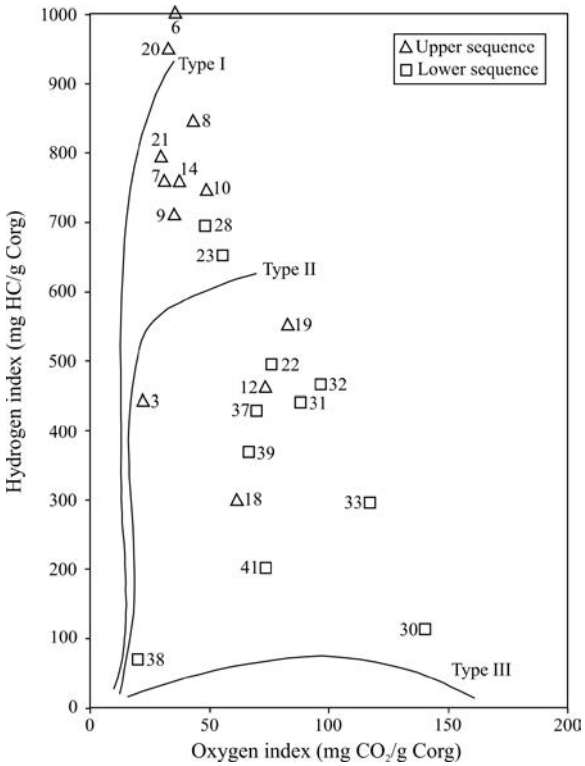

Fig. 5. Modified van Krevelen diagram Hydrogen Index (HI) *vs*. Oxygen Index (OI) (Langford and Blanc-Valleron, 1990).

in mineral proportions are followed by a notable change in the OM content. The elevated concentration of OM in the lower sequence, detected only in the depth interval 329 to 336 m (Table 4) can be related to coal layers (allochtonous OM, derived from the biomass of land plants), observed on a macroscopic scale during the sampling.

Table 4

Values of bulk organic geochemical parameters

Sequence	Description	No	Depth (m)	Corg (%)[1]	N (%)	S (%)	C/S[2]	C/N[3]	Bitumen (mg/g Corg)	HC[4] (mg/g Corg)	Asphaltenes + NSO[5] (mg/g Corg)
Clayey carbonates		1	11.5	10.64	0.31	0.97	29.28	40.03	117.11	3.44	113.67
Upper sequence (US)	Marly dolomite	2	13.5	4.13	0.16	0.38	29.02	30.10	334.79	5.69	329.10
		3	27	12.07	0.35	1.20	26.85	40.22	59.93	1.20	58.73
		4	32	4.01	0.16	0.37	28.93	29.23	112.89	2.61	110.29
		5	42.5	5.71	0.28	0.77	19.80	23.78	95.02	5.63	89.40
		6	54	11.04	0.44	1.05	28.07	29.26	134.26	7.56	126.70
		7	55.5	5.52	0.20	0.47	31.36	32.19	122.10	6.85	115.25
		8	64.5	3.03	0.07	0.24	33.71	50.48	78.35	4.67	73.68
	Marlstone, calcite dominated	9	70	4.72	0.14	0.78	16.16	39.32	111.41	5.90	105.51
		10	78	3.24	0.11	0.37	23.38	34.35	93.18	5.19	87.99
		11	80	5.78	0.17	0.57	27.07	39.65	124.6	5.69	118.91
		12	83	2.65	0.12	0.50	14.15	25.75	90.2	4.78	85.42
		13	96	3.62	0.16	0.76	12.72	26.38	80.93	3.70	77.23
		14	111	10.23	0.33	0.95	28.75	36.15	135.51	5.76	129.75
		15	113	1.58	0.11	0.70	6.03	16.75	136.27	5.44	130.83
		16	127	1.45	0.08	0.57	6.79	21.14	94.19	4.08	90.11
		17	137.5	6.30	0.20	0.75	22.43	36.73	74.38	3.17	71.21
		18	150	5.71	0.26	0.51	29.89	25.61	33.58	1.35	32.23
		19	164	1.71	0.07	0.31	14.73	28.49	88.03	4.14	83.89
		20	185	8.86	0.27	0.71	33.32	38.27	108.82	5.88	102.95
		21	189.5	5.81	0.23	0.61	25.43	29.46	31.87	1.37	30.51
Lower sequence (LS)	Marly laminated magnesite	22	216	1.42	0.06	0.15	25.27	27.60	183.71	8.08	175.63
		23	219	2.07	0.08	0.30	18.42	30.17	213.71	8.29	205.42
		24	224	0.32	0.10	0.56	1.53	3.73	276.69	13.56	263.13
		25	238	0.46	0.06	0.54	2.27	8.94	270.49	11.33	259.16
		26	243.5	2.14	0.08	0.50	11.43	31.2	213.75	10.58	203.17
		27	245	1.04	0.03	0.55	5.05	40.43	266.2	5.14	261.06
		28	248.3	3.02	0.09	0.48	16.80	39.13	329.45	10.51	318.94
		29	255	2.40	0.06	0.42	15.26	46.65	323.46	11.39	312.08
		30	258	0.81	0.07	1.83	1.18	13.49	158.19	5.33	152.86
		31	265	1.37	0.04	0.58	6.31	39.94	218.77	16.39	202.39
	Marly Mg dolomite, Silty Mg-marl-stone, Mg-clay	32	283	1.23	0.04	0.44	7.46	35.86	270.12	7.89	262.23
		33	286	0.88	0.03	0.60	3.92	34.21	262.38	12.10	250.28
		34	297.5	1.69	0.06	0.41	11.00	32.85	326.03	25.46	300.57
		35	309	0.51	0.04	0.97	1.40	14.87	251.39	10.26	241.13
		36	317.5	1.48	0.06	0.48	8.23	28.77	389.65	13.13	376.52
		37	324	2.08	0.08	0.83	6.69	30.32	336.19	17.25	318.95
		38	329	12.38	0.48	3.88	8.51	29.74	40.41	2.55	37.86
		39	335	4.50	0.20	0.30	40.05	26.24	81.17	4.69	76.48
		40	336	5.88	0.26	0.37	42.43	26.37	80.37	2.61	77.76
		41	340	2.69	0.12	1.37	5.24	26.14	89.33	4.63	84.70
		42	341	1.89	0.08	1.81	2.79	27.55	89.27	6.65	82.62
		43	343	0.77	0.06	2.50	0.82	14.97	81.95	3.96	77.99
Minimum US				1.45	0.07	0.24	6.03	16.75	31.87	1.20	30.51
Maximum US				12.07	0.44	1.20	33.71	50.48	334.79	7.56	329.1
Average US				5.36	0.20	0.63	22.93	31.67	107.02	4.53	102.48
Standard deviation US				3.09	0.10	0.25	8.48	7.85	61.50	1.82	60.54
Minimum LS				0.32	0.03	0.15	0.82	3.73	40.41	2.55	37.86
Maximum LS				12.38	0.48	3.88	42.43	46.65	389.65	25.46	376.52
Average LS				2.32	0.10	0.90	11.00	27.69	216.03	9.63	206.40
Standard deviation LS				2.61	0.10	0.89	11.66	10.76	102.01	5.49	98.04

[1] Corg – Organic carbon content; [2] C/S is given as molar ratio; [3] C/N is given as molar ratio; [4] HC – Content of saturated and aromatic hydrocarbons; [5] NSO – Polar compounds containing N, S and O.

Table 5

Results of Rock-Eval pyrolysis for selected samples

Sequence	Description	No	Depth (m)	S1[1] (mg HC [2]/g sample)	S2[3] (mg HC/g sample)	S3[4] (mg CO_2/g sample)	HI[5] (mg HC/ (g Corg)	OI[6] (mg CO_2/ g Corg)[5]	S2/S3	PI[7]	Tmax (°C)[8]
Upper sequence (US)	Marly dolomite	3	27	2.35	53.42	2.69	442.58	22.29	19.86	0.04	430
		6	54	7.78	112.31	3.93	1017.3	35.60	28.58	0.06	425
		7	55.5	3.51	41.96	1.73	760.14	31.34	24.25	0.08	430
		8	64.5	1.01	25.69	1.31	847.85	43.23	19.61	0.04	428
	Marlstone, calcite dominated	9	70	1.35	33.64	1.67	712.71	35.38	20.14	0.04	427
		10	78	0.63	24.21	1.57	747.22	48.46	15.42	0.03	429
		12	83	0.47	12.18	1.92	459.62	72.45	6.34	0.04	424
		14	111	2.84	77.74	3.81	759.92	37.24	20.40	0.04	430
		18	150	1.29	17.19	3.53	301.05	61.82	4.87	0.07	424
		19	164	0.38	9.44	1.41	552.05	82.46	6.70	0.04	427
		20	185	2.84	84.25	2.79	950.9	31.49	30.20	0.03	425
		21	189.5	0.95	46.21	1.73	795.35	29.78	26.71	0.02	429
Lower sequence (LS)	Marly laminated magnesite	22	216	0.47	7.08	1.10	498.59	77.46	6.44	0.06	452
		23	219	0.89	13.56	1.15	655.07	55.56	11.79	0.06	442
		25	238	0.24	1.41	0.95	306.52	206.52	1.48	0.15	423
		28	248.3	0.59	21.01	1.46	695.70	48.34	14.39	0.03	428
		30	258	0.16	0.93	1.14	114.81	140.74	0.82	0.15	434
		31	265	0.23	6.05	1.21	441.61	88.32	5.00	0.04	425
	Marly Mg dolomite, Silty Mg-marl-stone, Mg-clay	32	283	0.14	5.76	1.19	468.29	96.75	4.84	0.02	437
		33	286	0.10	2.62	1.04	297.73	118.18	2.52	0.04	445
		35	309	0.10	0.77	1.08	150.98	211.76	0.71	0.11	425
		37	324	0.26	8.98	1.47	432.77	70.84	6.11	0.03	439
		38	329	0.31	8.54	2.30	68.98	18.58	3.71	0.04	436
		39	335	0.17	16.72	3.00	371.56	66.67	5.57	0.01	442
		41	340	0.10	5.53	1.98	205.58	73.61	2.79	0.02	438
Minimum US				0.38	9.44	1.31	301.05	22.29	4.87	0.02	424
Maximum US				7.78	112.31	3.93	1017.3	82.46	30.20	0.08	430
Average US				2.12	44.85	2.34	695.56	44.29	18.59	0.04	427.33
Standard deviation US				2.07	32.01	0.97	215.12	18.60	8.69	0.02	2.35
Minimum LS				0.10	0.77	0.95	68.98	18.58	0.71	0.01	423
Maximum LS				0.89	21.01	3..00	695.7	211.76	14.39	0.15	452
Average LS				0.29	7.61	1.47	362.17	97.95	5.09	0.06	435.85
Standard deviation LS				0.23	6.23	0.60	196.17	57.99	4.07	0.05	8.67

[1] S1 – Free hydrocarbons; [2] HC – Hydrocarbons; [3] S2 – Pyrolysate hydrocarbons; [4] S3 – Amount of CO_2 generated from oxygenated functional groups; [5] HI – Hydrogen Index = S2 × 100/Corg; [6] OI – Oxygen Index = S3 × 100/Corg; [7] PI – Production Index = S1/(S1+S2); [8] Tmax – Temperature corresponding to S2 peak maximum.

Modified van Krevelen, Hydrogen Index (HI) *vs*. Oxygen Index (OI) diagram (Langford and Blanc-Valleron, 1990) shows that samples from the upper and lower sequence of the borehole ZLT-2, in addition to the OM content, also differ with regard to the OM type. The OM of sediments from the upper sequence comprises kerogen I/II, II, I and II/III types, whereas the OM of samples from the lower sequence consists of kerogen II/III, III and II types (Fig. 5).

There is no significant difference in sulphur content between samples (Table 4), although sediments from the lower sequence are generally enriched in this element. Higher concentrations of total organic carbon, accompanied by lower concentrations of sulphur, resulted in a notably higher C/S ratio in the upper sequence (Table 4).

Preferred utilization of carbon and bacterial fixation of nitrogen result in lowering of C/N values with increasing depth (Table 4), as it is reported for lacustrine sediments (Meyers and Ishiwatari, 1993).

The bitumen of all samples investigated is mainly represented by asphaltenes and polar-NSO compounds, whereas the relative amounts of saturated and aromatic hydrocarbons are low (Table 4), indicating low maturity. Values of Production Index (PI) lower than 0.1 confirms the low OM maturity (Table 5). Two samples have values of PI = 0.15. However, these samples contain low amounts of Corg (0.46% and 0.81%, respectively; Tables 4, 5) and therefore the Rock Eval parameters should be treated with caution (Kluska *et al*., 2013). The maximal temperature (T_{max}), which corresponds to S2 peak maximum, varies in a wide range (Table 5). However, this variation in T_{max} is related to different kerogen types, rather than to thermal maturity (Peters *et al*., 2005).

Table 6

Values of bulk organic geochemical parameters in liquid pyrolysates

Sample	Yield of liquid pyrolysates[1] (ppm)	Yield of liquid pyrolysates (mg/g Corg)	Yields of HC[2] (ppm)	Yields of HC (mg/g Corg)	Group composition of liquid pyrolysates		p_o[3] (bar)	P[4] (bar)
					Saturated + aromatic HC (%)	NSO + asphaltenes (%)		
3	4980	41.26	1796	14.88	36.07	63.93	5.0	5.9
6	13114	118.79	5996	54.31	45.72	54.28	4.9	5.5

[1] Relative to the bitumen-free sample; [2] HC – Hydrocarbons; [3] p_o – Initial pressure; [4] p – Pressure at the end of pyrolysis.

Characteristics of liquid pyrolysates – Bulk organic geochemical parameters

The generative potential of samples from the upper sequence, rich in organic matter containing kerogen I and II types, was investigated using conventional pyrolysis (Stojanović *et al*., 2010). Pyrolysis was performed on bitumen-free samples 3 and 6. Heated at 400°C for 4 hours, the bitumen-free samples generated a total liquid pyrolysate of 4980 ppm and 13114 ppm, and hydrocarbons of 1796 and 5996 ppm, respectively (Table 6). The yields are consistent with those of a source rock with good potential (Peters *et al*., 2005) and support the assumption, derived from elemental analysis and Rock-Eval pyrolysis of the initial samples (Tables 4, 5). Sample 6 showed a higher liquid hydrocarbons potential (Table 6), consistent with the Rock-Eval data (Table 5). Apart from the liquid pyrolysate, the pyrolytic experiments also produced gaseous products that may be generated by direct degradation of kerogen or as secondary products of the degradation of liquid hydrocarbons. The gaseous products were not analyzed. However, their presence is proved by measuring pressure in the autoclave at the end of pyrolysis, in relation to the initial pressure, which typically was ~5 bar (Table 6).

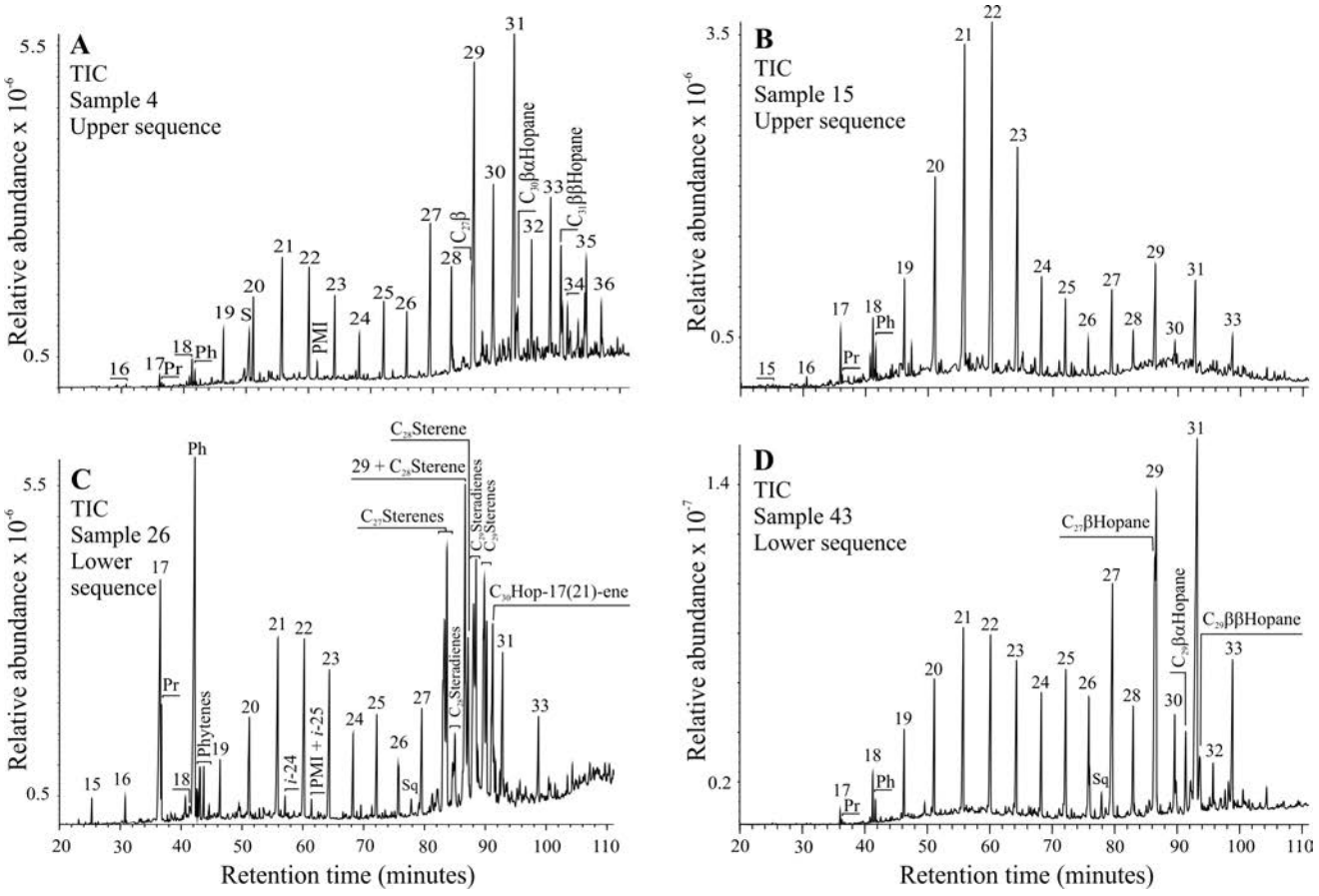

Fig. 6. Characteristic Total Ion Currents (TICs) of the saturated fractions in sedimentary rocks from the upper sequence (A, B) and the lower sequence (C, D). *n*-alkanes are labelled according to their carbon number; Pr – pristane; Ph – phytane; PMI – 2,6,10,15, 19-pentamethylicosane; *i*-24 – C_{24} regular isoprenoid; *i*-25 – C_{25} regular isoprenoid; Sq – squalane; S – sulphur; β designates configurations at C_{17} in hopanes; ββ and βα designate configurations at C_{17} and C_{21} in hopanes.

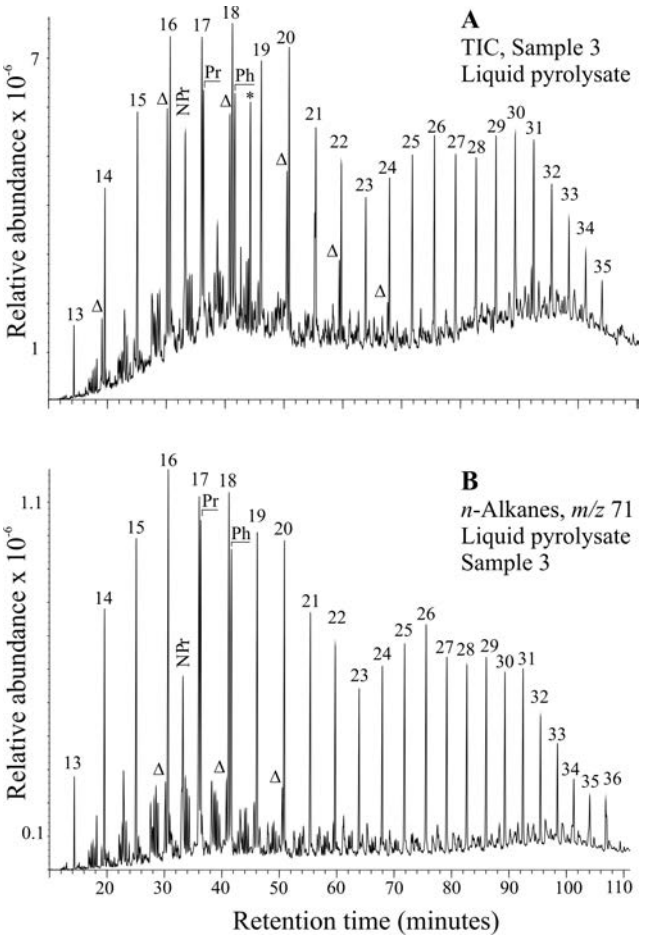

Fig. 7. Characteristic Total Ion Current (TIC) of the saturated fraction (**A**) and characteristic GC–MS chromatogram of *n*-alkanes (*m/z* 71) (**B**) in liquid pyrolysate. Δ – *n*-alkenes with same number of carbon atoms as *n*-alkanes; NPr – norpristane; * – phthalate contamination; for other peak assignments, see Fig. 6 legend.

Molecular composition of the organic matter

The total ion currents (TICs) of saturated fractions of the samples investigated are shown in Figure 6. The main constituents are *n*-alkanes, isoprenoids, and polycyclic alkanes with sterane and hopane skeleton. The *n*-alkanes are the predominant biomarkers in all the samples. However, samples showed differences with respect to *n*-alkane patterns and abundances of isoprenoids and steroids (Fig. 6), which were consistent with different OM types (Fig. 5).

The total ion currents (TICs) of saturated fractions of liquid pyrolysates were dominated by *n*-alkanes, typical of oil distribution, whereas *n*-alkenes were observed in low amounts (Fig. 7A).

n-Alkanes and acyclic isoprenoids

On the basis of *m/z* 71 mass chromatograms (Fig. 8), in almost all of the samples, *n*-alkanes are identified in the range C_{15} to C_{35} (Table 7). In all samples, the CPI values for the full range of *n*-alkanes (C_{16}–C_{34}) are higher than 2.4, indicating the significant predominance of odd-chain homologues (Table 7). CPI values for short-chain *n*-alkanes

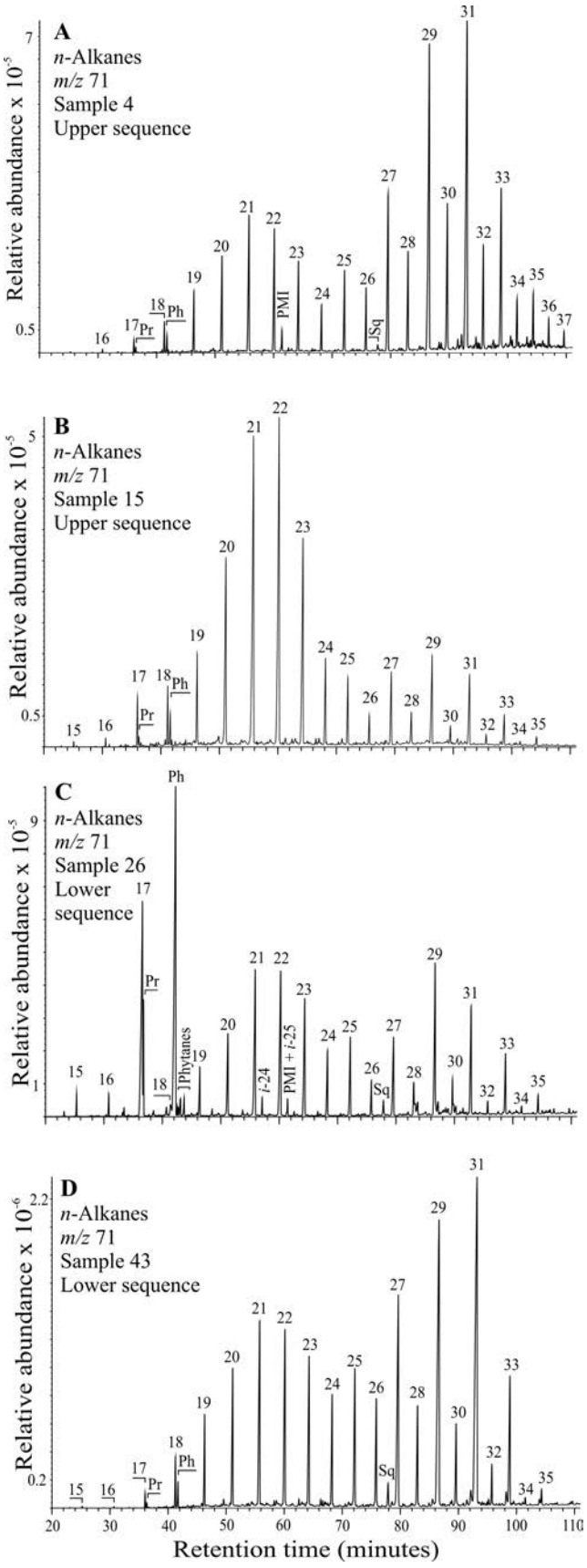

Fig. 8. Characteristic GC–MS chromatograms of *n*-alkanes (*m/z* 71) in sedimentary rocks from the upper sequence (**A**, **B**) and the lower sequence (**C**, **D**). For peak assignments, see Fig. 6 legend.

Table 7

Values of organic geochemical parameters calculated from the distributions and abundances of *n*-alkanes and isoprenoids

Sequence	Description	No	Depth (m)	*n*-Alkane range	CPI (C_{16}-C_{34})[1]	CPI (C_{16}-C_{24})[2]	CPI (C_{24}-C_{34})[3]	*n*-Alkane maximum	(C_{15}-C_{24})/(C_{25}-C_{35})[4]	LAD[5]	Pr[6]/Ph[7]	Pr/*n*-C_{17}	Ph/*n*-C_{18}
Clayey carbonates		1	11.5	16 - 35	4.92	2.15	5.61	C_{29}	0.34	1.21	0.20	0.54	1.06
Upper sequence (US)	Marly dolomite	2	13.5	15 - 35	4.53	2.05	5.08	C_{29}, C_{27}	0.47	1.15	0.33	0.26	0.60
		3	27	15 - 35	3.92	1.29	5.70	C_{31}, C_{29}	0.70	1.96	0.15	0.51	1.58
		4	32	16 - 37	2.94	1.28	3.11	C_{31}, C_{29}	0.29	3.28	0.35	0.52	0.60
		5	42.5	16 - 35	4.53	2.40	4.96	C_{27}, C_{29}	0.61	0.95	0.16	0.43	1.83
		6	54	15 - 35	5.58	2.86	6.21	C_{27}	0.40	0.98	0.25	0.37	1.38
		7	55.5	15 - 35	4.79	2.21	5.76	C_{31}, C_{23}	0.87	1.05	0.32	0.24	1.07
		8	64.5	15 - 35	2.58	1.34	3.20	C_{22}	2.47	0.67	0.66	0.48	0.39
	Marlstone, calcite dominated	9	70	15 - 35	3.47	1.97	3.68	C_{29}, C_{22}	0.77	1.02	0.18	0.40	1.60
		10	78	17 - 33	2.95	1.42	4.08	C_{22}	2.51	0.67	0.44	0.35	0.32
		11	80	14 - 33	2.79	1.23	3.91	C_{21}	1.39	0.91	0.40	0.41	0.68
		12	83	14 - 35	3.17	1.39	4.19	C_{22}, C_{21}	1.53	1.16	0.36	0.20	0.67
		13	96	14 - 35	3.33	1.26	5.56	C_{21}, C_{22}	1.63	1.64	0.23	0.15	0.78
		14	111	14 - 35	5.99	1.83	8.02	C_{31}	0.34	2.20	0.18	0.30	3.65
		15	113	15 - 35	2.57	1.29	2.83	C_{22}, C_{21}	3.43	0.65	0.33	0.22	0.59
		16	127	14 - 33	2.88	1.40	3.44	C_{22}, C_{21}	1.84	0.90	0.38	0.19	1.25
		17	137.5	16 - 35	6.16	1.93	7.32	C_{31}	0.28	2.68	0.18	0.77	3.47
		18	150	16 - 35	2.43	1.37	2.54	C_{22}, C_{21}	2.14	0.62	0.52	0.65	1.07
		19	164	15 - 35	3.86	2.48	3.98	C_{22}, C_{21}	2.56	0.44	0.30	0.37	1.07
		20	185	16 - 35	6.19	2.66	7.10	C_{29}, C_{31}	0.28	1.89	0.07	0.42	7.21
		21	189.5	16 - 35	4.85	1.78	5.92	C_{31}, C_{29}	0.44	1.91	0.08	0.32	3.76
Lower sequence (LS)	Marly laminated magnesite	22	216	15 - 35	2.47	1.33	2.81	C_{29}, C_{31}	0.79	1.12	0.49	0.94	2.41
		23	219	15 - 35	4.25	1.54	5.42	C_{31}, C_{29}	0.47	1.62	0.06	0.69	14.16
		24	224	15 - 35	3.72	1.80	4.27	C_{21}, C_{22}	1.02	1.00	0.11	0.25	3.15
		25	238	15 - 35	2.86	1.70	2.57	C_{22}	4.17	0.32	1.72	0.62	0.64
		26	243.5	15 - 35	4.32	2.69	3.88	C_{17}	1.62	1.13	0.14	0.22	25.72
		27	245	15 - 35	3.01	1.36	3.70	C_{22}, C_{21}	1.32	1.20	0.35	0.50	1.91
		28	248.3	15 - 35	2.91	2.72	2.37	C_{17}	0.99	1.71	0.25	0.17	4.04
		29	255	15 - 35	6.49	7.48	3.50	C_{17}	2.27	1.62	0.28	0.06	3.62
		30	258	15 - 35	4.66	2.15	5.64	C_{29}	0.67	1.44	1.24	0.38	1.99
		31	265	15 - 35	3.53	1.96	3.49	C_{22}, C_{21}	1.90	0.88	0.17	0.46	24.87
	Marly Mg dolomite, Silty Mg-marlstone, Mg-clay	32	283	15 - 35	3.79	1.57	4.55	C_{29}, C_{31}	0.75	1.61	0.40	0.53	3.18
		33	286	16 - 35	3.91	1.84	4.56	C_{29}, C_{22}	0.92	1.32	0.43	0.14	1.29
		34	297.5	15 - 33	3.40	2.12	3.29	C_{17}	1.38	1.40	2.17	1.39	3.87
		35	309	16 - 35	3.38	1.98	4.13	C_{17}	1.34	0.93	1.44	0.24	0.63
		36	317.5	16 - 35	2.50	1.41	3.21	C_{21}, C_{29}	1.27	0.92	0.52	0.82	2.20
		37	324	16 - 34	3.32	1.48	4.79	C_{29}	0.79	1.36	0.22	0.66	4.74
		38	329	16 - 35	3.54	1.51	5.10	C_{29}, C_{31}	0.90	1.04	0.10	0.56	6.89
		39	335	16 - 33	2.43	1.09	3.06	C_{29}, C_{31}	0.84	1.50	0.54	0.33	0.55
		40	336	16 - 33	5.10	1.80	8.45	C_{29}, C_{27}	0.75	1.02	0.6	0.31	0.45
		41	340	16 - 35	4.19	1.13	6.42	C_{31}, C_{29}	0.44	2.71	0.88	0.19	0.13
		42	341	15 - 35	4.06	1.27	5.68	C_{31}, C_{29}	0.54	2.25	0.33	0.45	0.39
		43	343	15 - 35	3.83	1.25	4.91	C_{31}, C_{29}	0.43	2.08	0.20	0.42	0.55
Minimum US					2.43	1.23	2.54		0.28	0.44	0.07	0.15	0.32
Maximum US					6.19	2.86	8.02		3.43	3.28	0.66	0.77	7.21
Average US					3.98	1.77	4.83		1.25	1.34	0.29	0.38	1.68
Standard deviation US					1.27	0.52	1.58		0.96	0.76	0.15	0.16	1.68
Minimum LS					2.43	1.09	2.37		0.43	0.32	0.06	0.06	0.13
Maximum LS					6.49	7.48	8.45		4.17	2.71	2.17	1.39	25.72
Average LS					3.71	1.96	4.36		1.16	1.37	0.57	0.47	4.88
Standard deviation LS					0.94	1.31	1.42		0.82	0.52	0.57	0.31	7.28

Table 8

Values of organic geochemical parameters calculated from the distributions and abundances of *n*-alkanes and isoprenoids in liquid pyrolysates

Sample	*n*-Alkane range	CPI (C_{16}-C_{34})	CPI (C_{16}-C_{24})	CPI (C_{24}-C_{34})	*n*-Alkane maximum	(C_{15}-C_{24})/(C_{25}-C_{35})	LAD	Pr/Ph	Pr/*n*-C17	Ph/*n*-C18
3	13 - 35	1.14	0.96	1.08	C_{16}, C_{17}	1.39	0.99	0.93	0.88	0.98
6	13 - 35	1.16	1.07	1.01	C_{16}, C_{17}	1.11	0.97	1.04	0.77	0.94

For abbreviations see Table 7 legend.

(C_{16}–C_{24}) range from 1.09 to 7.48, most probably resulting from relatively high contents of *n*-C_{17} and *n*-C_{21} (Fig. 8, Table 7). The CPI values for long-chain *n*-alkanes (C_{24}–C_{34}) are higher than 2.3 (Table 7). Average CPI values for three different ranges (full, short and long) are comparable, indicating uniform, low maturity level (Table 7). The samples investigated differ significantly according to *n*-alkane maxima and the distributions of *n*-alkanes, i.e. the abundance of short- and mid-chain homologues (C_{15}–C_{24}) *vs.* abundance of long-chain homologues (C_{25}–C_{35}; Table 7; Fig. 8).

Both pyrolysates have similar *n*-alkane distributions, in which the *n*-alkanes C_{16}–C_{20} are predominant, as is typical for aquatic organic matter (Fig. 7B). The CPI values for the three different ranges (full, short and long) for the pyrolysates are close to 1, which is typical of a mature oil distribution (Table 8).

The isoprenoids, pristane (Pr) and phytane (Ph), were identified in all samples (Figs 6, 8). Generally, higher values of Pr/Ph ratio, followed by more common variations of this parameter were observed in the lower sequence (Table 7). In samples from the lower sequence, the non-regular isoprenoid, squalane, C_{30}, was identified (Figs 6C, D, 8C, D). In the upper sequence, squalane is absent or present in very low amounts. The regular C_{24} isoprenoid was observed exclusively in sediments from depth interval 219–265 m (lower sequence, Figs 6C, 8C).

The C_{25} isoprenoid was observed only in samples from depths above 265 m, with values of the Pr/Ph ratio ≤ 0.35, (Figs 6A, C, 8A, C). Careful checking of the mass spectra (ratio of fragmentations ions, 239 and 253 as well as the abundance of fragmentation ion 113) of the corresponding peak (Vink *et al*., 1998; Peters *et al.*, 2005) showed that in the upper sequence, the peak represents the irregular C_{25} isoprenoid, 2,6,10,15,19-pentamethylicosane (PMI). In the sediments of the lower sequence, the peak is a mixture of regular and irregular C_{25} isoprenoids, with a dominance of the latter. The irregular PMI is related to methanogenic archaea (Schouten *et al*., 1997; Vink *et al*., 1998). The regular C_{25} isoprenoid is interpreted as an indicator of high salinity (Waples *et al*., 1974; Wang and Fu, 1997; Grice *et al*., 1998a, b; Yangming *et al*., 2005). However, the elevated content of the regular C_{25} isoprenoid was also identified in alkaline environments (Šajnović *et al*., 2008b). In addition it was reported that some families of methanogenic archaea (*Methanobacterium thermoautotrophicum*) also synthesize the precursor of the regular C_{25} isoprenoid (Risatti *et al*., 1984).

Unlike bitumen in the initial samples, squalane and PMI were absent from the liquid pyrolysates (Fig. 7). The values of Pr/Ph ratio were higher than in the initial bitumen (Tables 7, 8), which may be explained by the fact that the degradation of kerogen during laboratory simulations results in the uniform formation of both pristane and phytane (Stojanović *et al*., 2009, 2010).

Chromans

Alkylated 2-methyl-2-(4,8,12-trimethyltridecyl)chromans (MTTCs) were detected in aromatic fractions by ion chromatograms of *m/z* = 121 + 135 + 149 (Fig. 9). Samples from the lower sequence contained 8-methyl-MTTC, 5,8-dimethyl-MTTC, 7,8-dimethyl-MTTC and 5,7,8-trimethyl-MTTC (Fig. 9B), whereas in samples from the upper sequence only dimethyl- and trimethyl- MTTCs derivatives were observed (Fig. 9A). In all samples, 5,7,8-trimethyl-MTTC was the most abundant compound. On the basis of empirical observations, it was suggested by Sinninghe Damsté *et al*. (1989) that in sediments from non-hypersaline environments, 5,7,8-trimethyl-MTTC dominates and 8-methyl-MTTC is completely missing. Therefore, it might be assumed that samples from the upper sequence were deposited under non-saline conditions. For samples from the lower sequence, 5,7,8-trimethyl-MTTC was the most prominent compound, but 8-methyl-MTTC also occurred, which indicates certain differences in depositional environment between the sequences. For a more elaborate characterisation of palaeosalinities, the MTTC ratio was defined by Sinninghe Damsté *et al*. (1987, 1993) as MTTC ratio = 5,7,8-trimethyl-MTTC/total MTTCs (Table 9).

Chromans were not identified in the liquid pyrolysates.

Arylisoprenoids

In samples 3, 4, 14, 23, 26, 27, 28, 31 and 32, isoreniratane (I) and several other digenetic products of isoreniratene (II–X) are identified (Fig. 10).

Arylisoprenoids are absent from the liquid pyrolysates. This result is expected, owing to the sensitivity of their side chain to thermal stress.

CPI – Carbon Preference Index; [1] CPI (C_{16}-C_{34}) = 1/2 × [Σodd(*n*-C_{17} - *n*-C_{33})/Σeven(*n*-C_{16} - *n*-C_{32}) + Σodd(*n*-C_{17} - *n*-C_{33})/Σeven(*n*-C_{18} - *n*-C_{34})]; [2] CPI (C_{16}-C_{24}) = 1/2 × [Σodd(*n*-C_{17} - *n*-C_{23})/Σeven(*n*-C_{16} - *n*-C_{22}) + Σodd(*n*-C_{17} - *n*-C_{23})/Σeven(*n*-C_{18} - *n*-C_{24})]; [3] CPI (C_{24}-C_{34}) = 1/2 × [Σodd(*n*-C_{25} - *n*-C_{33})/Σeven(*n*-C_{24} - *n*-C_{32}) + Σodd(*n*-C_{25} - *n*-C_{33})/Σeven(*n*-C_{26} - *n*-C_{34})]; *n*-C_x designates *n*-alkane homologue, and x represents number of carbon atoms; [4] (C_{15}-C_{24})/(C_{25}-C_{35}) = [Σ(*n*-C_{15} - *n*-C_{24})/Σ(*n*-C_{25} - *n*-C_{35})]; [5] LAD = [Σ(*n*-C_{27} - *n*-C_{31})/Σ(*n*-C_{23} - *n*-C_{27})]; [6] Pr – Pristane; [7] Ph – Phytane.

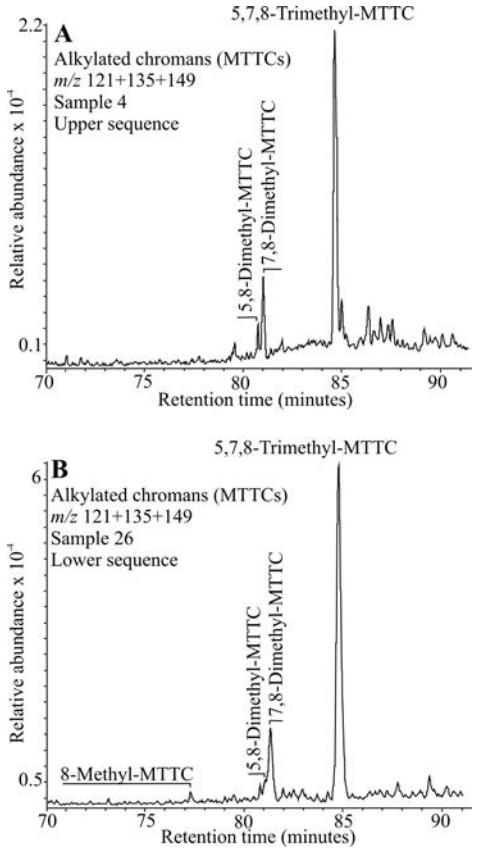

Fig. 9. Characteristic GC–MS chromatograms of MTTCs (*m/z* 121+135+149) in sedimentary rocks from the upper sequence (**A**) and the lower sequence (**B**).

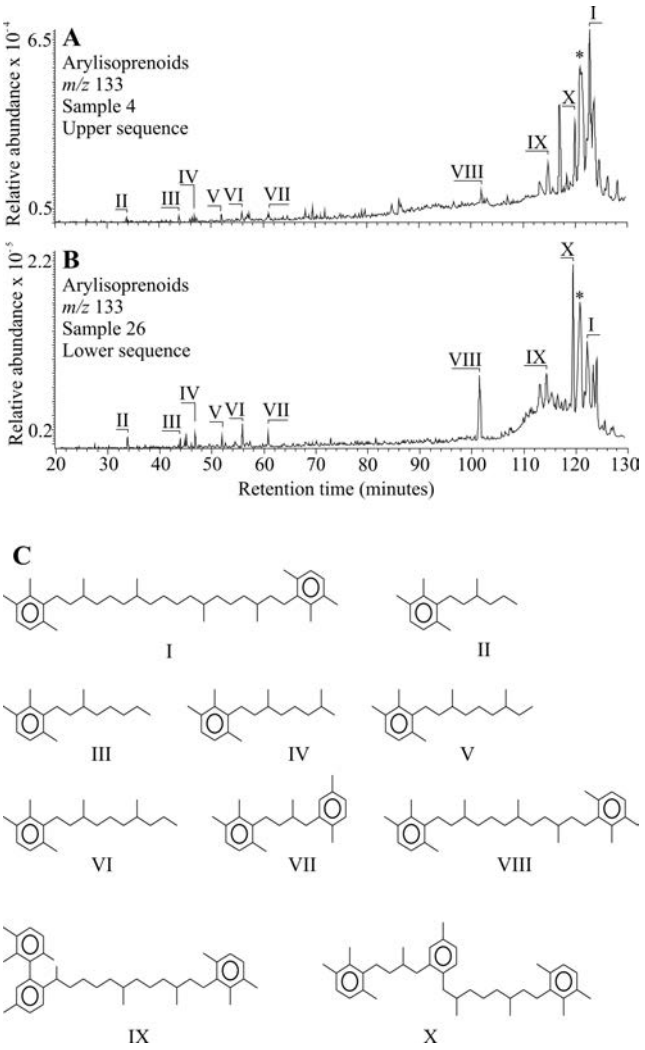

Fig. 10. Characteristic GC–MS chromatograms of arylisoprenoids (*m/z* 133) in sedimentary rocks from the upper sequence (**A**) and the lower sequence (**B**). **C.** The structures of arylisoprenoids identified in the samples. * Unidentified compound, M^+ 544?, basic ion, *m/z* 133.

Steroids and hopanoids

The distributions of steroid biomarkers are characterised by the presence of C_{27}–C_{29} saturated steranes with 5α(H)14α(H)17α(H) and 5β(H)14α(H)17α(H) 20R configurations, unsaturated sterenes in the same range with double bonds in the Δ^2, Δ^4 and Δ^5 positions, respectively, as well as steradienes (Fig. 11). A similar distribution of steroids was reported in Malm Zeta laminated carbonates from the Franconian Alb, SW Germany (Schwark *et al*., 1998). Thermodynamically more stable sterane isomers, with 5α(H)14α(H)17α(H) 20S and 5α(H)14β(H)17β(H) 20R or 20S configurations, are not present. Such steroid distributions indicate a low thermal maturity of the OM, consistent with the bitumen composition, PI and CPI discussed above (Tables 4, 5, 7). The sediments investigated are characterised by the dominance of C_{29} compounds or C_{27} compounds (Table 9), indicating a prevalence of terrestrial, or aquatic OM, respectively (Volkman, 1986), although elevated amounts of C_{29} steroids in samples containing kerogen I and I/II types (Fig. 5) also can be related to a contribution from green algae (Volkman, 2003). The main difference between sediments from the upper and lower sequences with regard to steroid biomarkers is expressed as elevated contents of C_{28} steroids in the lower sequence (Table 9).

[1] % C_{27} = 100 × C_{27}5α(H)14α(H)17α(H)-Sterane/[ΣC_{27}-C_{29} 5α(H)14α(H)17α(H)-Steranes]; [2] % C_{28} = 100 × C_{28}5α(H)14α(H)17α(H)-Sterane/[ΣC_{27}-C_{29} 5α(H)14α(H)17α(H)-Steranes]; [3] % C_{29} = 100 × C_{29}(5α(H)14α(H)17α(H)-Sterane/[ΣC_{27}-C_{29} 5α(H)14α(H)17α(H)-Steranes]; [4] ΔC_{27} = 100 × C_{27}(Δ^2 + Δ^4 + Δ^5)-Sterenes/[Σ(C_{27}-C_{29})(Δ^2 + Δ^4 + Δ^5)-Sterenes]; [5] ΔC_{28} Sterenes = 100 × C_{28}(Δ^2 + Δ^4 + Δ^5)-Sterenes/[Σ(C_{27}-C_{29})(Δ^2 + Δ^4 + Δ^5)-Sterenes]; [6] ΔC_{29} Sterenes = 100 × C_{29}(Δ^2 + Δ^4 + Δ^5)-Sterenes/[Σ(C_{27}-C_{29})(Δ^2 + Δ^4 + Δ^5)-Sterenes]; [7] Ster/Hop = [Σ(C_{27}-C_{29})(Δ^2 + Δ^4 + Δ^5)-Sterenes + Σ(C_{27}-C_{29})(5α(H)14α(H)17α(H) + 5β(H)14α(H)17α(H))-Steranes]/[Σ(C_{29}-C_{32})17α(H)21β(H)-Hopanes + Σ(C_{29}-C_{31})17β(H)21α(H)-Hopanes + Σ(C_{29}-C_{33}) 17β(H)21β(H)-Hopanes + C_{27}17α(H)-Hopane + C_{27}17β(H)-Hopane + C_{30}Hop-17(21)-ene + C_{27}Hop-17(21)-ene + C_{27}Hop-13(18)-ene + C_{30}Hop-13 (18)-ene]; [8] C_{30}ββ/C_{30}(ββ+αβ) = C_{30}17β(H)21β(H)-Hopane/(C_{30}17β(H)21β(H)-Hopane + C_{30}17α(H)21β(H)-Hopane); [9] C_{31}(S)/C_{31}(S+R) = C_{31} 17α(H) 21β(H)22(S)-Hopane/(C_{31}17α(H)21β(H)22(S)-Hopane + C_{31}17α(H)21β(H)22(R)-Hopane); [10] GI – Gammacerane Index = 100 × G/(G + C_{30}17α(H)21β (H)-Hopane); [11] MTTC - 2-Methyl-2-(4,8,12-trimethyltridecyl)chromans (MTTC) ratio = 5,7,8-Trimethyl-MTTC/(8-Methyl-MTTC + 5,8-Dimethyl-MTTC + 7,8-Dimethyl-MTTC + 5,7,8-Trimethyl-MTTC); 12 N.D. - Not determined due to the absence of steranes, sterenes, C_{31}17α(H)21β(H)22(S)-hopane and gammacerane. For sample 34 parameters calculated from the distributions of steroids and hopanoids are missing.

Table 9

Values of organic geochemical parameters calculated from the distributions and abundances of steroids, hopanoids and chromans

Sequence	Description	No	Depth (m)	% C_{27} [1]	% C_{28} [2]	% C_{29} [3]	% ΔC_{27} [4]	% ΔC_{28} [5]	% ΔC_{29} [6]	Ster/Hop [7]	$C_{30}\beta\beta/C_{30}(\beta\beta+\alpha\beta)$ [8]	$C_{31}(S)/C_{31}(S+R)$ [9]	GI [10]	MTTC [11]
Clayey carbonates		1	11.5	27.32	29.16	43.52	23.45	27.81	48.75	0.11	0.82	N.D.	N.D.	0.79
Upper sequence (US)	Marly dolomite	2	13.5	34.78	20.72	44.50	49.89	18.24	31.87	0.06	0.75	N.D.	N.D.	0.75
		3	27	34.12	16.69	49.19	35.52	14.82	49.66	0.24	0.76	N.D.	N.D.	0.82
		4	32	32.36	15.68	51.96	26.90	15.13	57.97	0.20	0.83	N.D.	N.D.	0.79
		5	42.5	26.78	20.39	52.82	32.08	21.17	46.76	0.14	0.82	0.06	N.D.	0.81
		6	54	N.D. [12]	N.D.	N.D.	27.93	15.28	56.80	0.20	0.84	N.D.	N.D.	0.84
		7	55.5	N.D.	N.D.	N.D.	30.04	9.46	60.50	0.32	0.80	0.10	N.D.	0.82
		8	64.5	21.21	9.23	69.57	20.26	7.80	71.94	0.13	0.75	0.12	N.D.	0.76
	Marlstone, calcite dominated	9	70	N.D.	N.D.	N.D.	26.14	14.60	59.26	0.09	0.79	0.15	N.D.	0.82
		10	78	32.73	19.78	47.49	27.00	17.17	55.83	0.17	0.74	0.17	N.D.	0.84
		11	80	34.72	19.77	45.50	32.84	15.63	51.54	0.34	0.72	0.04	N.D.	0.83
		12	83	42.55	18.26	39.20	50.62	16.42	32.96	0.30	0.47	N.D.	17.14	0.63
		13	96	40.14	12.40	47.47	59.47	13.23	27.30	0.31	0.46	N.D.	33.52	0.79
		14	111	51.45	7.86	40.69	42.48	10.62	46.90	0.30	0.56	N.D.	23.68	0.75
		15	113	25.52	18.08	56.40	38.34	1.82	59.84	0.46	0.39	N.D.	5.95	0.86
		16	127	52.57	15.42	32.00	N.D.	N.D.	N.D.	0.18	0.39	N.D.	N.D.	0.67
		17	137.5	N.D.	N.D.	N.D.	32.63	13.71	53.66	0.18	0.74	N.D.	N.D.	0.71
		18	150	N.D.	N.D.	N.D.	32.63	9.85	57.51	0.44	0.71	N.D.	N.D.	0.50
		19	164	43.24	15.76	41.00	48.92	12.01	39.07	0.30	0.75	N.D.	N.D.	0.74
		20	185	N.D.	N.D.	N.D.	48.28	10.11	41.62	0.56	0.87	0.17	N.D.	0.80
		21	189.5	N.D.	N.D.	N.D.	40.90	12.68	46.42	0.47	0.77	N.D.	N.D.	0.81
Lower sequence (LS)	Marly laminated magnesite	22	216	26.52	51.92	21.56	36.88	40.49	22.63	0.58	0.51	0.25	13.73	0.72
		23	219	N.D.	N.D.	N.D.	66.29	13.04	20.67	0.35	0.84	N.D.	67.08	0.82
		24	224	N.D.	N.D.	N.D.	53.83	15.83	30.34	0.31	0.80	N.D.	63.09	0.78
		25	238	25.98	29.68	44.35	N.D.	N.D.	N.D.	0.48	0.11	0.15	12.31	0.61
		26	243.5	N.D.	N.D.	N.D.	41.79	25.56	32.65	3.64	0.68	0.14	45.00	0.77
		27	245	48.78	25.20	26.02	47.15	30.62	22.22	0.27	0.86	N.D.	30.44	0.78
		28	248.3	51.35	24.54	24.11	36.22	14.45	49.33	0.55	0.79	N.D.	37.10	0.81
		29	255	25.36	42.10	32.55	29.84	35.87	34.30	0.71	0.81	N.D.	55.76	0.78
		30	258	29.52	36.50	33.98	27.65	31.32	41.03	0.60	0.69	0.30	24.95	0.71
		31	265				27.51	17.54	54.95	5.02	0.57	0.31	24.52	0.79
	Marly Mg dolomite, Silty Mg-marlstone, Mg-clay	32	283	37.80	26.96	35.24	47.12	26.54	26.33	0.48	0.73	N.D.	40.45	0.69
		33	286	31.60	22.15	46.24	27.11	42.68	30.21	0.51	0.66	N.D.	35.04	0.58
		34	297.5	N.D.	N.D.	N.D.	N.D.	N.D.	N.D.	N.D.	N.D.	N.D.	N.D.	0.73
		35	309	32.40	33.47	34.13	N.D.	N.D.	N.D.	0.23	0.44	N.D.	8.77	0.61
		36	317.5	43.01	30.62	26.37	53.44	22.50	24.06	0.53	0.64	N.D.	N.D.	0.60
		37	324	42.69	29.45	27.86	43.45	27.73	28.81	0.74	0.72	N.D.	62.01	0.70
		38	329	34.90	40.20	24.91	41.40	30.77	27.84	1.44	0.66	N.D.	37.85	0.71
		39	335	11.91	9.91	78.18	17.08	9.37	73.55	0.18	0.83	N.D.	N.D.	0.63
		40	336	8.28	8.41	83.31	9.55	8.04	82.41	0.45	0.74	N.D.	23.55	0.61
		41	340	7.29	21.98	70.73	5.67	11.84	82.49	0.19	0.83	N.D.	N.D.	0.67
		42	341	9.72	19.87	70.41	N.D.	N.D.	N.D.	0.11	0.78	N.D.	22.32	0.57
		43	343	12.55	15.90	71.55	11.46	6.90	81.64	0.08	0.74	0.16	N.D.	0.43
Minimum US				21.21	7.86	32.00	20.26	1.82	27.30	0.06	0.39	0.00	0.00	0.50
Maximum US				52.57	20.72	69.57	59.47	21.17	71.94	0.56	0.87	0.21	33.52	0.86
Average US				36.32	16.16	47.52	36.99	13.14	49.86	0.27	0.70	0.05	4.01	0.77
Standard deviation US				9.44	10.35	11.28	10.22	7.42	12.67	0.15	0.15	0.07	9.43	0.09
Minimum LS				7.29	8.41	21.56	5.67	6.90	20.67	0.08	0.11	0.00	0.00	0.43
Maximum LS				51.35	51.92	83.31	66.29	42.68	82.49	5.02	0.86	0.31	67.08	0.82
Average LS				28.22	27.58	44.20	34.64	22.84	42.53	0.83	0.69	0.06	28.76	0.69

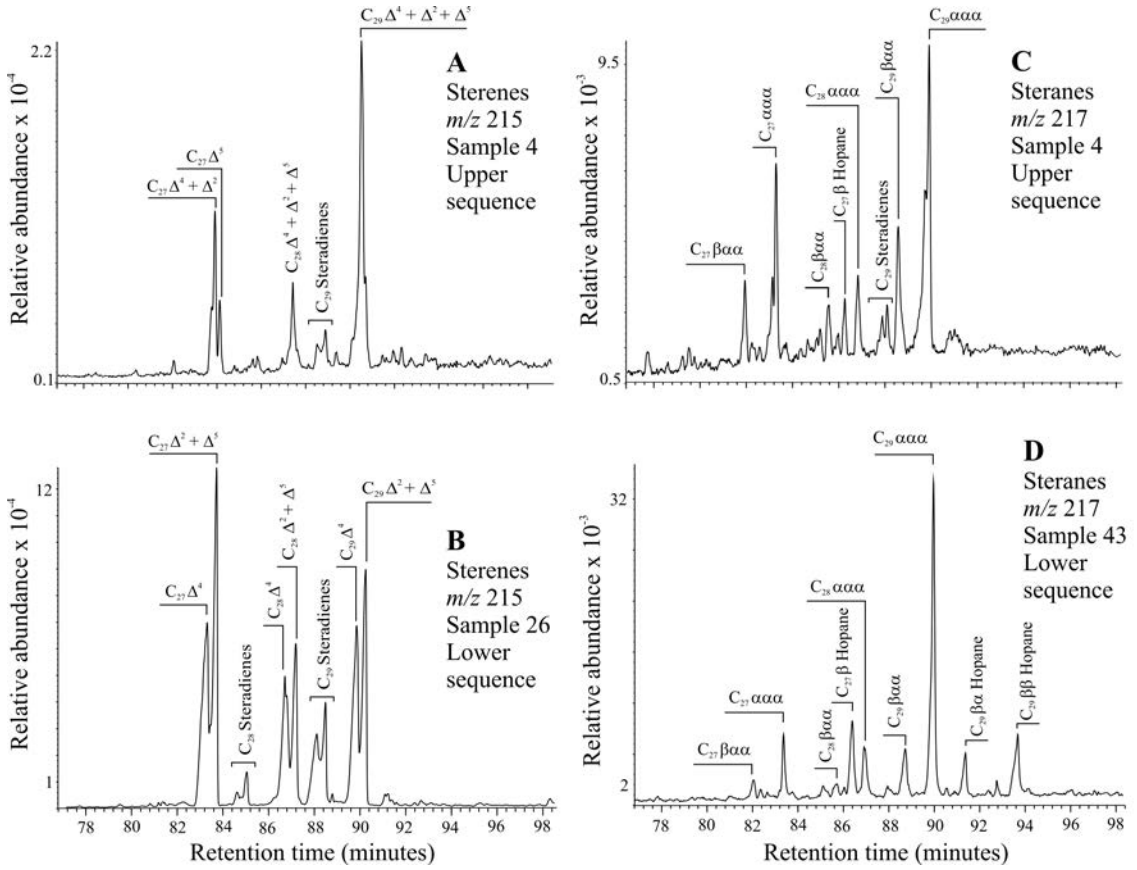

Fig. 11. Characteristic GC–MS chromatograms of sterenes, *m/z* 215 (**A**, **B**) and steranes, *m/z* 217 (**C**, **D**) in sedimentary rocks from the upper sequence and the lower sequence. Δ^2, Δ^4 and Δ^5 designate double bonds in positions 2, 4 and 5 in sterenes; ααα and βαα designate configurations at C_5, C_{14} and C_{17} in 20(R) steranes.

The sterane distributions in pyrolysates obtained at 400°C are typical for oils (Fig. 12A), which confirms the good potential of the sediments investigated and shows that catagenesis was simulated successfully by pyrolysis. Apart from the regular 5α(H)14α(H)17α(H)20(R)-steranes, C_{27}–C_{29} isomers with thermodynamically more stable 5α(H)14α(H)17α(H) 20(S)-, 5α(H)14β(H)17β(H)20(R)-, and 5α(H)14β(H)17β(H) 20(S)-configurations, as well as the typical geoisomers, βα- and αβ-diasteranes, were present (Fig. 12A). As in bitumen of initial samples 3 and 6, C_{27} and C_{29} steranes are more abundant in liquid pyrolysates than C_{28} homologues (Tables 9 and 10). Values of the most used sterane maturation parameters based on the ratios of C_{29} sterane isomers, C_{29}αββ(R)/(C_{29}αββ(R)+ααα(R)) and C_{29}ααα(S)/C_{29}ααα(S+R) in all pyrolysates are lower than equilibrium values (Peters *et al*., 2005; Table 10).

On the basis of a mass chromatogram, *m/z* 191 of the saturated fractions, the hopane composition is characterised by the presence of C_{27}–C_{32} 17α(H)21β(H), C_{29}–C_{31} 17β(H) 21α(H), and C_{27}–C_{33} 17β(H)21β(H) compounds with the exception of C_{28} homologues in all three series (Fig. 13). Other hopanoid-type constituents of the saturated fraction are C_{27} hop-13(18)-ene and C_{27} hop-17(21)-ene, whereas C_{30} hop-17(21)-ene was observed in samples from the lower sequence (depth interval 219–265 m). The presence of unsaturated hopenes, the dominance of ββ-isomers over αβ-hopanes and the complete absence of αβ-22(S) isomers or low values of C_{31}(S)/(S+R) ratio (< 0.3) confirm an immature

Table 10

Values of organic geochemical parameters calculated from the distributions and abundances of steranes and hopanes in liquid pyrolysates

Sample	% C_{27}	% C_{28}	% C_{29}	C_{29}αααα(S)/ C_{29}αααα(S+R)	C_{29}αββ(R)/ (C_{29}αββ(R)+αααα(R))	C_{31}(S)/ C_{31}(S+R)	C_{29}βα/C_{29}αβ	C_{30}βα/C_{30}αβ	Ts/(Ts+Tm)[2]
3	33.78	29.68	36.54	0.50	0.55	0.58	0.29	0.35	0.42
6	31.83	29.96	38.21	0.49	0.54	0.57	0.36	0.44	0.41
E.V.				0.52–0.55	0.67–0.71	0.57–0.62		0.15[1]	

[1] – For samples of Tertiary age; [2]Tm – C_{27}17α(H)-22,29,30-trisnorneohopane; for other abbreviations see Table 9 and Figure 12 legend.

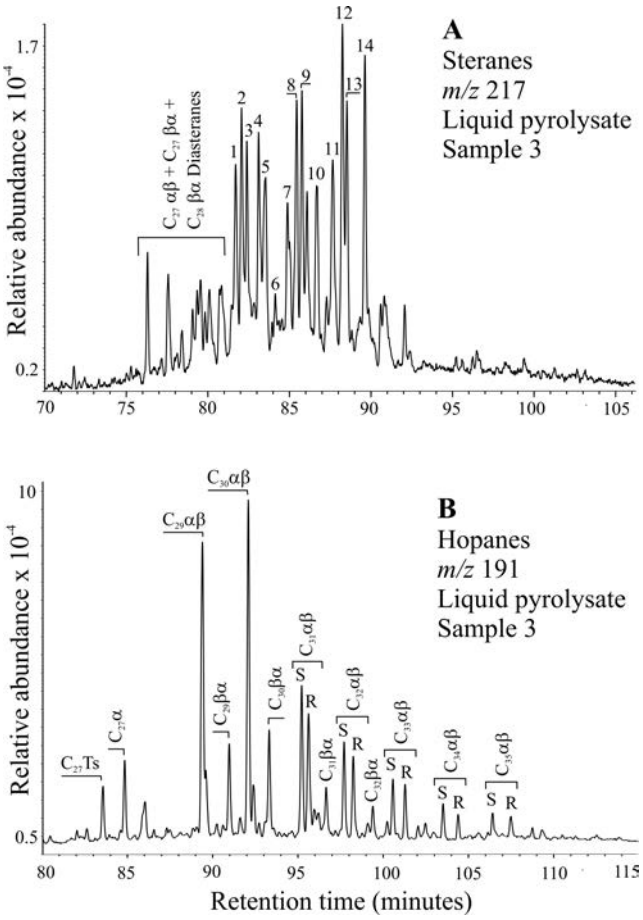

Fig. 12. Characteristic GC–MS chromatograms of steranes, *m/z* 217 (**A**) and hopanes, *m/z* 191 (**B**) in liquid pyrolysate. 1 – $C_{27}5\alpha(H)14\alpha(H)17\alpha(H)20(S)$-sterane + $C_{28}13\alpha(H)17\beta(H)20(S)$-diasterane; 2 – $C_{27}5\alpha(H)14\beta(H)17\beta(H)20(R)$-sterane + $C_{29}13\alpha(H)17\alpha(H)20(S)$-diasterane; 3 – $C_{27}5\alpha(H)14\beta(H)17\beta(H)20(S)$-sterane + $C_{28}13\alpha(H)17\beta(H)20(R)$-diasterane; 4 – $C_{27}5\alpha(H)14\alpha(H)17\alpha(H)20(R)$-sterane; 5 – $C_{29}13\alpha(H)17\alpha(H)20(R)$-diasterane; 6 – $C_{28}5\alpha(H)14\alpha(H)17\alpha(H)20(S)$-sterane; 7 – $C_{29}13\alpha(H)17\beta(H)20(S)$-diasterane; 8 – $C_{28}5\alpha(H)14\beta(H)17\beta(H)20(R)$-sterane + $C_{29}13\alpha(H)17\beta(H)20(R)$-diasterane; 9 – $C_{28}5\alpha(H)14\beta(H)17\beta(H)20(S)$-sterane; 10 – $C_{28}5\alpha(H)14\alpha(H)17\alpha(H)20(R)$-sterane; 11 – $C_{29}5\alpha(H)14\alpha(H)17\alpha(H)20(S)$-sterane; 12 – $C_{29}5\alpha(H)14\beta(H)17\beta(H)20(R)$-sterane; 13 – $C_{29}5\alpha(H)14\beta(H)17\beta(H)20(S)$-sterane; 14 – $C_{29}5\alpha(H)14\alpha(H)17\alpha(H)20(R)$-sterane; β and α designate configurations at C_{17} in hopanes; ββ, βα and αβ designate configurations at C_{17} and C_{21} in hopanes; Ts – $C_{27}18\alpha(H)$-22,29,30-trisnorneohopane; (S) and (R) designate configuration at C_{22} in hopanes.

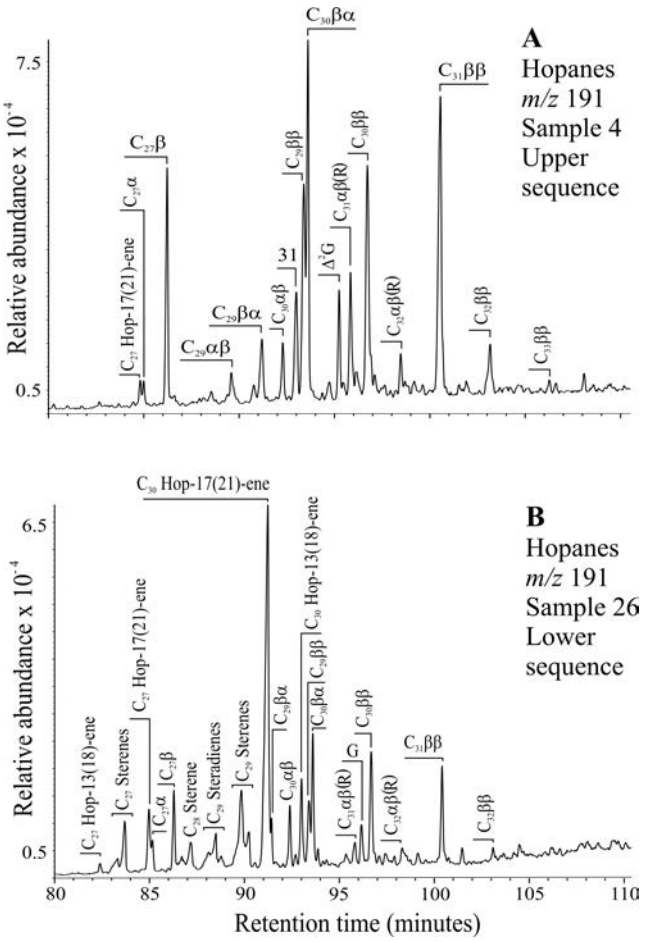

Fig. 13. Characteristic GC–MS chromatograms of hopanoids (*m/z* 191) in sedimentary rocks from the upper sequence (**A**) and the lower sequence (**B**). Δ^2G – 2-gammacerene; G – gammacerane; for other peak assignments, see Fig. 12 legend.

stage for the OM (Table 9; Fig. 13). The absence of C_{34} and C_{35} hopanes could be explained by the high sensitivity of the side chains from biologic hopanoids, which were readily degraded in the upper, oxygenated part of the stratified water column and/or to the lower contribution of those bacteria that synthesise bacteriohopanetetrol.

Gammacerane was identified in the majority of samples from the lower sequence and in several samples from the upper sequence. Its precursor, 2-gammacerene, formed by the dehydration of tetrahymanol (Peters *et al*., 2005), is present in almost all of the samples (Fig. 13).

Both pyrolysates contain a greater quantity of thermodynamically more stable C_{29} and C_{30} αβ-hopanes, compared to the corresponding βα-moretanes ($C_{29}\beta\alpha/C_{29}\alpha\beta$ and $C_{30}\beta\alpha/C_{30}\alpha\beta$ below 1; Table 10), whereas unstable ββ-hopanes and unsaturated hopenes were not identified (Fig. 12B). On the basis of the mass spectra of the corresponding peaks, Ts and the 22R and 22S epimers of C_{31}–C_{35} homohopanes were determined in the pyrolysates (Fig. 12B). Values for $C_{31}(S)/C_{31}(S+R)$-homohopanes indicated that in isomerisation 22(R) → 22(S) equilibria had been achieved in both pyrolysates; which is established in the earliest phase of catagenesis, at vitrinite reflectance, Ro ≈ 0.60 (Peters *et al*., 2005; Table 10). This result, together with the appearance of the hopane distribution in the liquid pyrolysates (ion fragmentogram *m/z* 191; Fig. 12B), which is typical for mature source rocks and oils, provide proof that catagenesis using pyrolysis at 400°C was simulated successfully and confirms the good potential of the samples investigated.

Alkylnaphthalenes and alkylphenanthrenes

The main constituents of the aromatic fractions of the liquid pyrolysates are alkylnaphthalenes and alkylphenanthrenes, which showed distributions typical for mature source rocks and oils (Fig. 14). The values of the corresponding maturity ratios are given in Table 11.

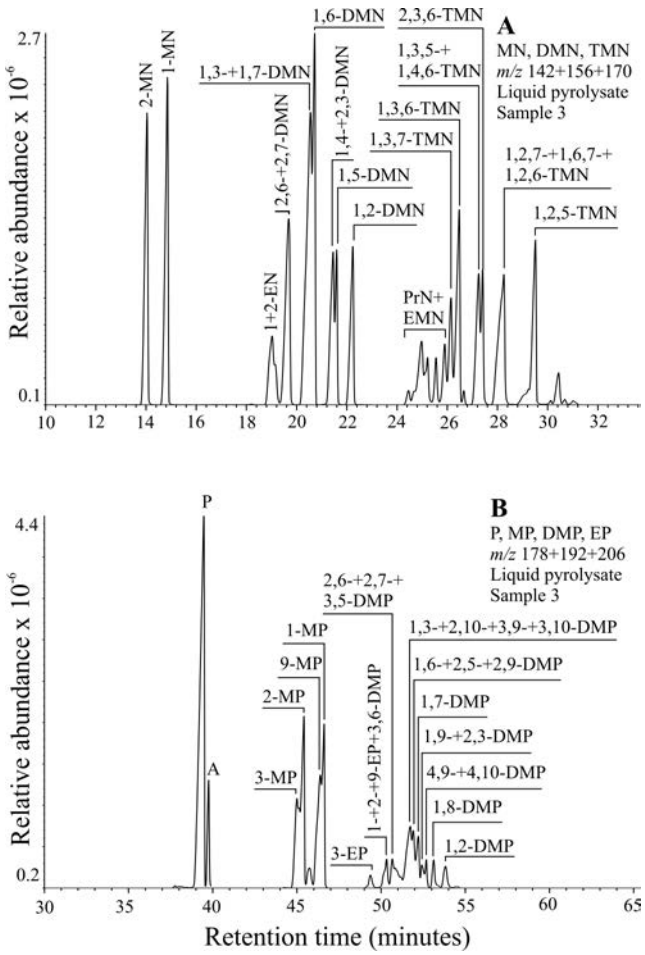

Fig. 14. Characteristic GC-MS chromatograms of (**A**) MN, DMN and TMN (*m/z* 142 + 156 + 170), and (**B**) P, MP and DMP (*m/z* 178 + 192 + 206) in liquid pyrolysate. MN – methylnaphthalene; DMN – dimethylnaphthalene; TMN – trimethylnaphthalene; PrN – propylnaphthalene; EMN – ethylmethylnaphthalene; P – phenanthrene; A – anthracene; MP – methylphenanthrene; DMP – dimethylphenanthrene; EP – ethylphenanthrene.

DISCUSSION

Mineral composition and geochemistry

The entire section studied belongs to an intrabasinal lacustrine facies, although Mg-clays at the bottom of the basin fill indicate a marginal sedimentary environment. The lower sequence of the intrabasinal facies (216–343 m) is most probably more marginal, but that cannot be strictly defined on the basis of only one borehole core. In general, in this lower sequence, sedimentation occurred in shallow water with the predominant Mg ions derived from ultramafic rocks, while sedimentation of the upper sequence occurred in slightly deeper water, with predominant Ca ions (Fig. 15; Table 1). The higher variations of the Sr and Na_2O contents in the lower sequence, compared to the upper sequence of the core studied (Fig. 16; Tables 1, 2), indicates more variable sedimentary conditions at the beginning of basin evolution, i.e. the formation of Mg-clays and marly magnesite, and rare thin (up to 2 mm) layers with dissolved, readily soluble minerals in the lower sequence of the intrabasinal facies (Fig. 17). Pronounced volcanic activity, evidenced by several tuff layers, influenced lower the palaeoproductivity and/or preservation of the organic matter (Fig. 2).

The significant positive correlation between B and Na_2O contents (Fig. 18) indicates that the high boron concentrations in the lower sequence of the intrabasinal facies (Table 3) are most probably related to searlesite, identified by XRD analyses (Fig. 3C). This result is consistent with an earlier study of the Kremna Basin (Živković and Stojanović, 1976), which reported the presence of searlesite. The presence of boron minerals in the Kremna Basin was interpreted as hydrothermal in origin (Ilić, 1969; Obradović *et al*., 1996). However, boron rich sediments also can originate from diagenetic processes in tuffaceous sediments in saline-alkaline lakes (Sheppard and Gude, 1973; Stamatakis, 1989; Šajnović *et al.*, 2008b). In arid areas, boron is likely to be co-precipitated with Mg and Ca hydroxides as coatings on the sediment particles and it also may occur as Na-metaborate (Floyd *et al*., 1998; Alonso, 1999).

The upper sequence of the intrabasinal facies (13.5–216 m) was deposited in slightly deeper water, with predominant Ca ions (Table 1), resulting in the formation of more

Table 11

Values of organic geochemical parameters calculated from distributions and abundances of naphthalene and phenanthrene hydrocarbons in liquid pyrolysates

Sample	MNR[1]	DMNR[2]	DNx[3]	α/βDN 1[4]	TNR 1[5]	TNR 2[6]	TMNR[7]	TNy[8]	MPI 1[9]	MPI 3[10]	Rc[11]	DMPI 1[12]	DMPI 2[13]	PAI 1[14]	PAI 2[15]	DBT/P[16]
3	0.93	0.32	2.79	1.04	0.63	0.56	0.35	2.05	0.55	1.06	0.73	0.45	0.35	1.08	0.71	0.16
6	1.11	0.40	2.57	0.93	0.61	0.71	0.61	1.71	0.56	1.06	0.74	0.65	0.38	1.14	0.86	0.14

[1]MNR = 2-MN/1-MN (Radke *et al.*, 1982b); [2]DMNR = (2,6-+2,7-DMN)/(1,4-+1,5-+1,6-+2,3-+2,6-+2,7-DMN) (Yawanarajah and Kruge, 1994); [3]DNx = (1,3-+1,6-+1,7-DMN)/(1,4-+1,5-+2,3-DMN) (Stojanović *et al.*, 2007); [4]α/ DN 1 = (1,4-+1,5-+2,3-DMN)/(2,6-+2,7-DMN) (Golovko, 1997); [5]TNR 1 = 2,3,6-TMN/(1,3,5-+1,4,6-TMN) (Alexander *et al.*, 1985); [6]TNR 2 = (1,3,7-+2,3,6-TMN)/(1,3,5-+1,3,6-+1,4,6-TMN) (Radke, 1987); [7]TMNR = 1,3,7-TMN/(1,3,7-+1,2,5-TMN) (van Aarssen *et al.*, 1999); [8]TNy = (1,3,6-+1,3,7-TMN)/(1,3,5-+1,4,6-TMN) (Stojanović *et al.*, 2007); [9]MPI 1 = 1.5 × (2-+3-MP)/(P+1-+9-MP) (Radke *et al.*, 1982a) ; [10]MPI 3 = (2-+3-MP)/(1-+9-MP) (Radke, 1987) ; [11]Rc = 0.6 MPI 1 + 0.37 (Radke and Welte, 1983); [12]DMPI 1 = 4 × (2,6-+2,7-+3,5-+3,6-DMP+1-+2-+9-EP)/(P+1,3-+1,6-+1,7-+2,5-+2,9-+2,10- +3,9- +3,10-DMP) (Radke *et al.*, 1982a); [13]DMPI 2 = (2,6-+2,7-+3,5-DMP)/(1,3-+1,6-+2,5-+2,9-+2,10-+3,9-+3,10-DMP) (Radke *et al.*, 1982b); [14]PAI 1 = (1-+2-+3-+9-MP)/P (Ishiwatari and Fukushima, 1979); [15]PAI 2 = ΣDMP/P (Ishiwatari and Fukushima, 1979); [16]DBT/P = Dibenzothiophene/Phenanthrene (Hughes *et al.*, 1995); MN – Methylnaphthalene; DMN – Dimethylnaphthalene; TMN – Trimethylnaphthalene; P – Phenanthrene; MP – Methylphenanthrene; DMP – Dimethylphenanthrene; EP – Ethylphenanthrene.

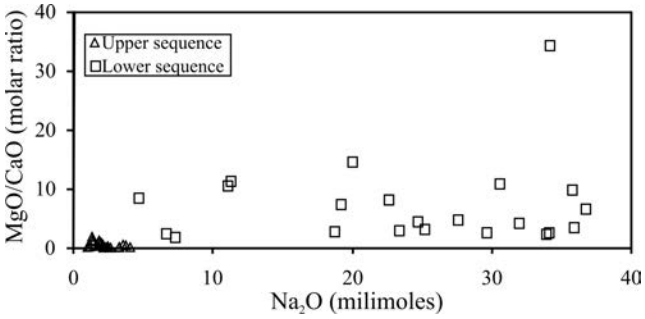

Fig. 15. Correlation diagram MgO/CaO *vs*. Na_2O.

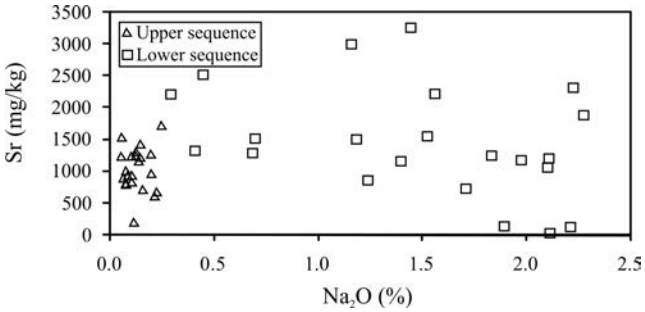

Fig. 16. Correlation diagram Sr *vs*. Na_2O.

uniform marlstone and dolomite (Figs 2, 3A). The rare volcanic input and stable sedimentary conditions were responsible for the higher productivity and better preservation of the organic matter.

Content and precursors of the organic matter

Lower sequence. The lower sequence contains lower amounts of total and soluble OM (Tables 4, 5). The OM of these sediments is composed of kerogen II/III, III and II types (Fig. 5). This result indicates a significant contribution of the allochtonous biomass of land plants from the lake catchment to the OM of the sediments, particularly in the lower part of the sequence (265–343 m). The relatively low OM content could be attributed to a lower palaeoproductivity (i.e. *in situ* OM production) and/or more intense degradation (i.e. a higher redox potential in the environment).

Samples from the lower part of the lower sequence are characterised by the dominance of odd long-chain *n*-alkane homologues C_{27}–C_{31}, a $(C_{15}–C_{24})/(C_{25}–C_{35})$ ratio < 1 and the prevalence of C_{29} homologues in the C_{27}–C_{29} sterane and sterene distributions (Tables 7, 9; Figs 8D, 11D), indicating significant input of terrestrial OM (Bray and Evans, 1961; Volkman, 1986; Cranwell *et al*., 1987). Samples from upper part of the lower sequence (219–265 m, an interval of chemical precipitation of carbonates) are characterised by *n*-alkane maxima at C_{17}, C_{21} or C_{22}, $(C_{15}–C_{24})/(C_{25}–C_{35})$ > 1 and a ratio of C_{27}/C_{29} steranes and sterenes > 1 (Tables 7, 9; Figs 8C, 11B), implying dominance of aquatic OM (Neto *et al*., 1998; Peters *et al*., 2005).

The identification of PMI in samples with Pr/Ph ≤ 0.35 (Figs 6C, 8C) indicates methanogenic archaea as the precursor of the OM (Rissati *et al*., 1984; Schouten *et al*., 1997).

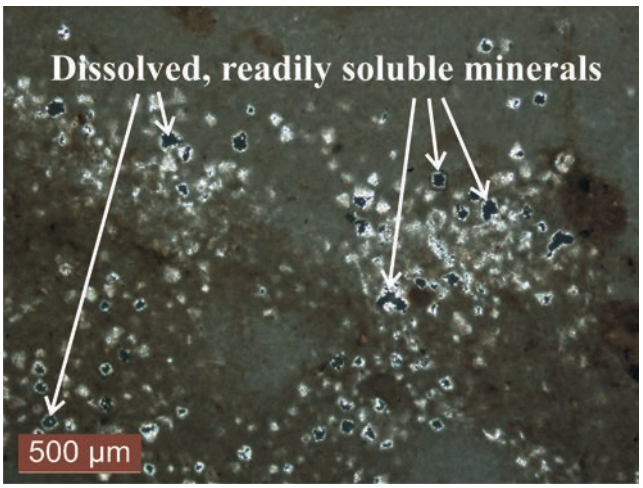

Fig. 17. Thin-section image of layers with dissolved, readily soluble minerals in the lower sequence of the intrabasinal facies (sample 26).

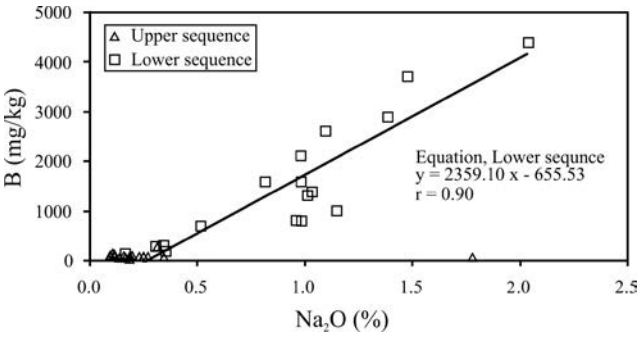

Fig. 18. Correlation diagram B *vs*. Na_2O.

The regular C_{25} isoprenoid is a common indicator of elevated salinity (Waples *et al*., 1974; Wang and Fu, 1997; Grice *et al*., 1998a, b; Yangming *et al*., 2005). However, the presence of this biomarker in the lower sequence in part also may be related to the methanogenic archaea *Methanobacterium thermoautotrophicum*, which synthesize C_{25} alkenes, the hydrogenation of which results in the formation of the regular C_{25} isoprenoid. The presence of phytenes in these samples (Figs 6C, 8C) corroborates the previous assumption, as it was reported that *Methanobacterium thermoautotrophicum* also synthesizes C_{20} alkenes with a phytene skeleton (Rissati *et al.*, 1984).

Isorenieratene (I; see Fig. 10C for structures) is a carotenoid, uniquely biosynthesized by the brown-coloured strains of the photosynthetic green sulphur bacterium (*Chlorobiaceae*). In samples (23, 26, 27, 28, 31 and 32), isorenieratane, the hydrogenated counterpart of isorenieratene and other diagenetic products of isorenieratene were identified (II–X, Fig. 10B, C). Although isorenieratane also can originate from β-carotene (Koopmans *et al*., 1996b), a widespread carotenoid synthesized by algae, bacteria and land plants (Peters *et al*., 2005), the presence of other diagenetic products of isorenieratene (II–X; Fig. 10B) uniquely indicates the contribution of a photosynthetic green sulphur bacterium (*Chlorobiaceae*) to the precursor OM. It also

should be noted that the diagenetic products of β-carotene, such as β-carotane and other derivatives with the prominent typical fragmentation ions *m/z* 119 and 120 (Koopmans *et al*., 1997), were absent.

The main precursor of 2-gammacerene and gammacerane is tetrahymanol. The principal source of tetrahymanol appears to be bacterivorous ciliates, which occur at the interface between oxic and anoxic zones in stratified water columns. Moreover, tetrahymanol was reported in ferns (Zander *et al*., 1969), an anaerobic rumen fungus (Kemp *et al*., 1984) and photosynthetic bacteria (Kleeman *et al*., 1990). Considering the previous discussion, the presence of 2-gammacerene and gammacerane in the samples investigated partly can be related to bacterivorous ciliates. In several ciliates, C_{30} hopan-3-β-ol was also identified. Therefore, it is reasonable to speculate that the abundant C_{27}, C_{29} and C_{30} hopanoids with ββ-configuration in the samples studied (Fig. 13), could be attributed at least to some extent to ciliate sources.

Abundant hopanoid biomarkers (ster/hop ratio < 1 in the majority of the samples; Table 9) indicate a significant contribution of prokaryotic organisms to the sedimentary OM. This result is consistent with the significant proportion of kerogen II type in the OM (Fig. 5) and the conclusions drawn by Bohacs *et al*. (2000, 2003).

Bacteriohopanetetrol with minor contribution of 3-desoxyhopanes from prokaryotes and fungi, are considered as the main biological precursors of geohopanoids (Ourisson *et al*., 1979; Rohmer *et al*., 1992). In addition, Chaffee *et al*. (1986) reported that hopanes containing less than 30 carbon atoms could originate from ferns, lichens and mosses. Elevated amounts of hopanoids with less than 30 carbon atoms (Fig. 13), observed in some samples, may also signify methanotrophic bacteria (e.g., *Methylococcus capsulatus* or *Methylomonas methanica*, which synthesized aminobacteriohopanepentol; Neunlist and Rohmer, 1985), as a source of the OM. These bacteria had suitable conditions, owing to the presence of methanogenic archaea (see the discussion related to the irregular C_{25} isoprenoid, PMI), which produce methane as a source of methanotrophics.

C_{30} Hop-17(21)-ene was detected in samples 20–32, with the exception of sample 22 (Fig. 13B). According to Bottari *et al*. (1972) and Volkman *et al*. (1986), C_{30}hop-17(21)-ene is introduced into sediments by bacteria or in some cases of ferns and mosses, whereas Brassell *et al*. (1980) suggest a diagenetic origin from the transformation of hop-22(29)-ene (diploptene). Wolff *et al*. (1992) suggest sulphate-reducing bacteria as a probable source of C_{30}hop- 17(21)-ene.

Upper sequence. The upper sequence is relatively rich in OM that comprises kerogen I/II, II, I and II/III types (Tables, 4, 5). Samples from this sequence are characterised by the dominance of C_{21} and C_{22} *n*-alkanes or long-chain odd homologues in the range C_{27} to C_{33}, and the predominance of either C_{27} or C_{29} homologues in the C_{27}–C_{29} steroid distribution (Tables 7, 9; Figs 8A, B, 11A, C). *n*-Alkane (C_{15}–C_{24})/(C_{25}–C_{35}) ratio vary in a wide range of 0.28–3.43 (Table 7). These data indicate mixed aquatic/terrestrial OM sources (Peters *et al*., 2005).

Although the *n*-alkane distributions of samples 3, 6, 14, 20 and 21 show maxima at odd long-chain homologues and have CPI and (C_{15}–C_{24})/(C_{25}–C_{35}) values > 1 (Table 7), Rock Eval data suggest kerogen I and I/II types (Fig. 5; Table 5). In addition to an origin from higher land plants, there are reports of C_{27}–C_{31} *n*-alkanes originating from strains of *Botryococcus braunii* race A (e.g., Moldowan *et al*., 1985; Derenne *et al*., 1988) by the reduction of the *n*-alkadienes and trienes they biosynthesized (e.g., Banerjee *et al*., 2002, and references therein). Therefore, it can be assumed that the green unicellular microalga, *Botryococcus braunii* race A was the source of the OM in the sediments of the upper sequence. For purpose of quantification of the variability of the long chain *n*-alkanes, Kluska *et al*. (2013) proposed novel parameter, the LAD (long *n*-alkane distribution) ratio. This ratio includes range of *n*-alkanes which are considered typical for *Botryococcus braunii* race A. For the samples mentioned (3, 6, 14, 20 and 21) this ratio varies in the range 0.98 to 1.96 (Table 7). These values are similar to those observed during an investigation of sediments from the Werra cyclothem (Upper Permian, Fore-Sudetic Monocline, Poland), for which *Botryococcus braunii* race A also was proposed as a source of the OM (Kluska *et al*., 2013). The significant contribution of a green alga is further supported by the high relative abundance of C_{29} steroid homologues, observed in these samples (Fig. 11A, Table 9).

The identification of PMI in samples with values of the Pr/Ph ratio ≤ 0.35, indicates methanogenic archaea as precursors of the OM (Risatti *et al*., 1984; Schouten *et al*., 1997; Vink *et al*., 1998). In samples 3, 4 and 14, isorenieratane and other diagenetic products of isorenieratene were identified (Fig. 10A), indicating a photosynthetic green sulphur bacterium (*Chlorobiaceae*) as an OM source.

The presence of gammacerane and 2-gammacerene (Fig. 13) partly can be related to bacterivorous ciliates (Peters *et al*., 2005), whereas abundant hopanoid biomarkers indicate a significant contribution from prokaryotic organisms (possibly including methanotrophic bacteria, owing to elevated amounts of C_{27} to C_{30} hopanes, Fig. 13A; Neunlist and Rohmer, 1985) to the sedimentary OM.

Characteristics of depositional environment

Lower sequence. The pristane to phytane ratio is widely used as indicator of redox settings (Didyk *et al*., 1978). However, it also depends on thermal maturity and increases with thermal alteration of the OM. Low values of this ratio (< 0.8) were also reported in hypersaline environments (ten Haven *et al*., 1987; Peters *et al*., 2005). On the basis of the amounts of NSO compounds in bitumen, values of PI, CPI, and biomarker maturity parameters (Tables 4, 5, 7 and 9), the influence of thermal maturity on this sample set could be ruled out. On the other hand, the distributions of MTTCs (Fig. 9B) and the values of the MTTC ratio (Table 9) show that there are no indications of hypersalinity. Therefore, a Pr/Ph ratio lower than 1 (with exception of 4 samples, Table 7) could imply sedimentation under reducing conditions. The plot Pr/*n*-C_{17} *vs*. Ph/*n*-C_{18} ratio (Shanmugam, 1985) corroborates the previous assumption (Fig. 19).

The higher amount of C_{28} homologue in the distribution of C_{27}–C_{29} steroids (Fig. 11B; Table 9; Volkman 1986;

Wang and Fu, 1997) , the presence of squalane, C_{24} and C_{25} regular isoprenoids (Fig. 6C; Waples, 1974; Grice *et al*., 1998a, b), the higher values of GI (Table 9; Peters *et al*., 2005) and the distribution of MTTCs (Fig. 9B; Sinninghe Damsté *et al*., 1987, 1993), followed by elevated MgO/CaO ratio and elevated content of Na_2O (Fig. 15; Table 1), indicate that sediments from lower sequence were deposited under alkaline conditions. Similar conditions were established during the investigation of the Lower Miocene lacustrine Valjevo-Mionica Basin, located close to the Kremna Basin (Šajnović *et al*., 2008a, 2009), and the Piskanja borate deposit, Jarandol Basin, Serbia (Szabó *et al*., 2009).

The presence of gammacerane, 2-gammacerene (Fig. 13), MTTCs and isoreniratene diagenetic products (Figs 9B, 10B) implies stratification of the water column (Sinninghe Damsté *et al*., 1995). The presence of isoreniratene diagenetic products (Fig. 10B) indicates a photic zone of anoxia (Koopmans *et al*., 1996a; Kluska *et al*., 2013), characterised by periods when the water column was highly stratified and anoxic waters extended up into the photic zone.

Upper sequence. Considering that there was no influence of hypersalinity and maturity, the Pr/Ph ratio < 1 (Table 7) and plot Pr/*n*-C_{17} *vs*. Ph/*n*-C_{18} (Fig. 19; Shanmugam, 1985) implies reducing conditions.

Generally, the lower values of Pr/Ph ratio in the upper sequence, followed by less variation of this parameter, indicate more reductive settings, i.e. deposition under a higher water column by comparison with sediments from the lower sequence (Table 7). This result could imply higher precipitation that is consistent with the palaeoclimate reconstruction obtained from an investigation of the palaeoflora in Serbia, which showed that during the Lower Miocene, precipitation rates increased, peaking in the Eggenburgian/Ottnangian (Utescher *et al*., 2007). Therefore, a higher amount of OM (Tables 4, 5) in sediments from the upper sequence to some extent could be related to more reducing conditions (resulting from a deepening of the water column), which contributed to better OM preservation.

The low amounts of Na_2O (Fig. 15; Table 1) and the C_{28} homologue in the distribution of C_{27}–C_{29} steranes and sterenes (Table 9; Fig. 11A, C), the absence of or trace amounts of squalane, the absence of C_{24} and C_{25} regular isoprenoids (Fig. 6A, B), the distribution of MTTCs (Fig. 9A) along with the dominance of calcite as the primary carbonate and the low MgO/CaO ratio (Figs 2A, 15) show that sediments from the upper sequence were formed in a freshwater environment.

The presence of 2-gammacerene (Fig. 13A), MTTCs (Fig. 9A) and isoreniratene diagenetic products (Fig. 10A) implies that stratification of the water column (Sinninghe Damsté *et al*., 1995; Kluska *et al*., 2013) resulted from temperature differences within the higher water column. A photic zone of anoxia is also indicated.

Investigation of the liquid hydrocarbon generation potential and assessment of the conditions for achieving early catagenesis

The yields of total liquid pyrolysate of 4980 and 13114, and hydrocarbons of 1796 ppm and 5996 ppm, respectively (Table 6) indicate a good generation potential for the organic-rich sediments of the upper sequence (samples 3 and 6). Liquid pyrolysates have typical oil distributions of biomarkers (*n*-alkanes, steranes, hopanes; Figs 7, 12) and alkylaromatics (Fig. 14), which confirms the good potential of the sediments investigated and shows that catagenesis was simulated successfully by pyrolysis.

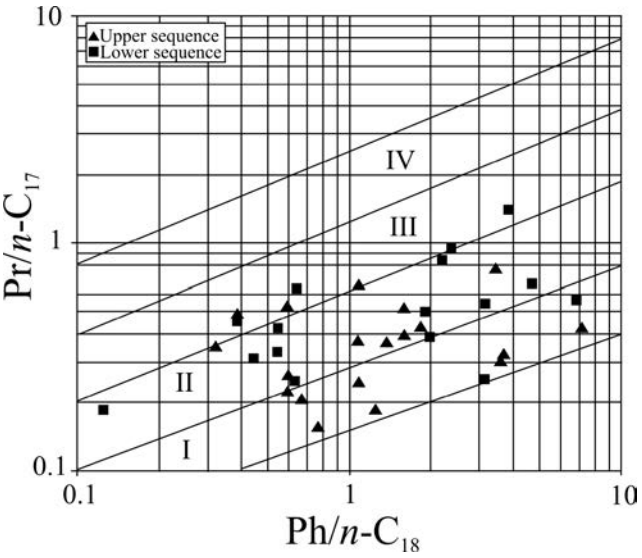

Fig. 19. Plot of Pr/*n*-C_{17} *vs*. Ph/*n*-C_{18} (Shanmugam, 1985). I – Algal OM, reducing environments; II – Mixed OM, reducing and transitional environments; III – Peat-coal environments; IV – Terrestrial OM, oxic environments.

Values for C_{31}(S)/C_{31}(S+R)-homohopanes indicate that in isomerisation 22(R) → 22(S) the equilibria was achieved in liqiud pyrolysates; established in the earliest phase of catagenesis, at vitrinite reflectance ≈ 0.60 (Peters *et al*., 2005; Table 10). On the other hand, the values of sterane maturation parameters, $C_{29}\alpha\beta\beta$(R)/($C_{29}\alpha\beta\beta$(R)+$\alpha\alpha\alpha$(R)) and $C_{29}\alpha\alpha\alpha$(S)/$C_{29}\alpha\alpha\alpha$(S+R) in pyrolysates are lower than the equilibrium values (Peters *et al*., 2005; Table 10). Bearing in mind that in the previous studies it was noticed that equilibria in the sterane isomerisations are established at vitrinite reflectance value of approximately 0.80% and taking into consideration the fact that equilibria were attained in homohopane isomerisations 22(R) → 22(S) in both pyrolysates (Table 10), it may be assumed that during pyrolysis at 400°C the sample investigated reached an equivalence value of vitrinite reflectance between 0.60 and 0.80% (Peters *et al*., 2005).

The low dibenzothiophene/phenanthrene ratio (DBT/P; Table 11) confirms formation of the sediments of the upper sequence in a freshwater environment. The values of naphthalene and phenanthrene maturity ratios in pyrolysates are similar and in a range that is typical for oils (Table 11). Applying the equation Rc = 0.6 MPI 1 + 0.37 (Radke and Welte, 1983), the vitrinite reflectance equivalent (Rc) of 0.70% for pyrolysates of at 400°C was calculated (Table 11). This Rc value is in full agreement with the results, obtained in the interpretation of the terpane and sterane biomarkers (Table 10).

Therefore, it can be assumed that pyrolysis of the samples investigated at 400°C achieved oil generation at a vitrinite reflectance equivalent of ~ 0.70%. Applying a generalized diagram that relates vitrinite refelectance, depth and a

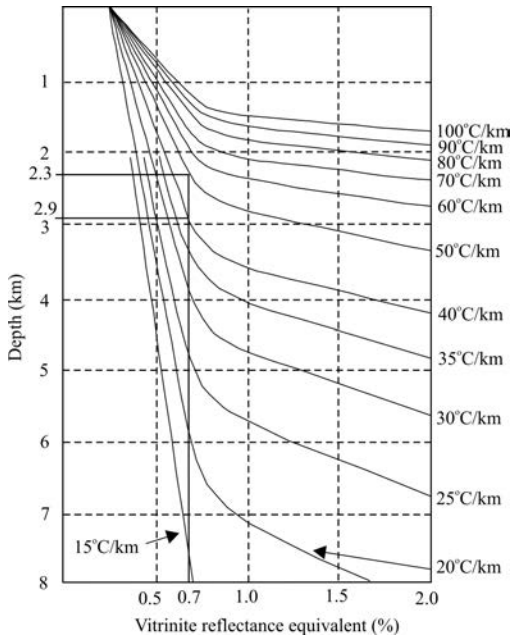

Fig. 20. Depth *vs*. vitrinite reflectance *vs*. geothermal gradient (according to Suggate, 1998); % of Rc values, calculated in this study, and corresponding depths are indicated.

regional geothermal gradient (Suggate, 1998) of between 40 and 50°C/km (Kostić, 2010), the minimum depth of 2300–2900 m was estimated, as that at which the sediments would become a thermally mature source rock (Fig. 20). The minimum temperature necessary for catagenetic generation of hydrocarbons (temperature = depth x geothermal gradient + annual mean surface temperature; Suggate, 1998) was calculated at 103°C (t = 2.3 × 40 + 11 = 103°C). Using the basin-independent equation T = (lnRo+1.68)/0.0124 (Barker & Pawlewicz, 1994) and a vitrinite reflectance, Ro, value of 0.70%, the temperature is estimated to be 107°C. The estimated temperature for hydrocarbon generation and the necessary depth are in good agreement with corresponding data for the active source rocks in the region (Dragaš *et al.*, 1991; Jovančićević *et al.*, 2002; Kostić, 2010; Mrkić *et al*., 2011).

CONCLUSIONS

Lacustrine sediments of the Kremna Basin (borehole ZLT-2, at depths of up to 343 m) originated from an ultramafic source. One main intrabasinal facies with two sequences was distinguished. The lower sequence occurs at depths of 216–343 m, while the upper sequence is encountered from 13.5–216 m. The sediments contain variable amounts and types of immature OM.

A comprehensive analysis of the OM indicates diverse precursors: bacteria, algae and, terrestrial plants. A higher contribution of allochtonous biomass of land plants from the lake catchment is observed in the sediments of the lower part of the lower sequence (265–343 m). Biomarker distributions reveal the following possible sources of the OM in the stratified water column: methanogenic archaea, a photosynthetic green sulphur bacterium (*Chlorobiaceae*), bacterivorous ciliates, various bacteria (photosynthetic and non-photosynthetic), and the green unicellular microalga, *Botryococcus braunii* race A (strictly in the upper sequence).

At the beginning of basin development (216–343 m), sedimentation took place in shallow water. This lower sequence consists of Mg-rich sediments with lower amounts of OM. Indications of volcanic activity include tuff layers and the presence of searlesite. The OM of these sediments is composed of kerogen II/III, III and II types. Through time, a slight deepening of basin occurred. This was followed by deposition of Ca-rich sediments (depth interval 13.5–216 m). These sediments are richer in OM, which comprises kerogen I/II, II, I and II/III types.

A higher water level (more reducing conditions) contributed to better OM preservation and also resulted in an elevated content of autochthonous aquatic OM in the sediments of the upper sequence. The transition between the lower and upper sequences is associated with a decrease of MgO/CaO ratio, a decrease of Na_2O and B contents, and an increase in the OM content. The main differences between the sequences with regard to biomarker distribution are expressed in the more uniform and lower Pr/Ph ratio, the lower amounts of C_{28} steroids and gammacerane index, the absence or significantly lower amount of squalane, the absence of 8-methyl-MTTC, C_{24} and C_{25} regular isoprenoids, as well as C_{30} hop-17(21)-ene in the sediments of the upper sequence.

The liquid pyrolysate and hydrocarbons yields obtained in the pyrolitic experiments, the distributions of saturated biomarkers and the alkylaromatics in pyrolysates supported the assumption, derived on the basis of the Rock-Eval data and the analysis of the initial bitumen, that the samples of the upper sequence, rich in OM in its catagenetic phase, could be a source of liquid hydrocarbons. The values of hopane, sterane and phenanthrene maturation parameters indicate that through pyrolysis at 400°C the samples investigated reached a value of vitrinite reflectance, equivalent to approximately 0.70%. It was estimated that the sediments investigated should occur at depths of 2300–2900 m to become active source rocks. The calculated minimum temperature, necessary for catagenetic hydrocarbon generation, is between 103 and 107°C.

Acknowledgments

The investigations that formed this study were done in cooperation with the company, Rio Tinto – Rio Sava Exploration, from Serbia. The study was partly financed by the Ministry of Education, Science and Technological Development of the Republic of Serbia (Projects 176006 and 176016). The authors are also grateful to Bartosz Budzyń (Polish Academy of Sciences, Kraków, Poland), Ladislav Palinkaš (University of Zagreb, Zagreb, Croatia) and two anonymous reviewers, whose helpful suggestions and comments greatly benefited this paper.

REFERENCES

Alexander, R., Kagi, R. I., Rowland, S. J., Sheppard, P. N. & Chirila, T. V., 1985. The effects of thermal maturity on distributions of dimethylnaphthalenes and trimethylnaphthalenes in some ancient sediments and petroleums. *Geochimica et*

Cosmochimica Acta, 49: 385–395.

Alonso, R. N., 1999. On the origin of La Puna Borates. *Acta Geologica Hispanica (Geologica Acta)*, 34: 141–166.

Banerjee, A., Sharma, R., Chisti, Y. & Banerjee, U. C., 2002. *Botryococcus braunii*: a renewable source of hydrocarbons and other chemicals. *Critical Reviews in Biotechnology,* 22: 245–279.

Barker, C. E. & Pawlewicz, M. J., 1994. Calculation of vitrinite reflectance from thermal histories and peak temperatures. a comparison of methods. In: Mukhopadhyay, P. K. & Dow, W. G. (eds), *Vitrinite Reflectance as a Maturity Parameter: Applications and Limitations*. American Chemical Society, Washington, D.C., pp. 216–222.

Bohacs, K. M., Carroll, A. R. & Neal, J. E., 2003. Lessons from large lake systems-Thresholds, nonlinearity, and strange attractors. In: Chan, M. A. & Archer, A. W. (eds), *Extreme Depositional Environments: Mega End Members in Geologic Time. Geological Society of America Special Papers*, 370: 75-90.

Bohacs, K. M., Carroll, A. R., Neal, J. E. & Mankiewicz, P. J., 2000. Lake-basin type, source potential, and hydrocarbon character: an integrated sequence stratigraphic geochemical framework. In: Gierlowski-Kordesch, E. H. & Kelts, K. R. (eds), *Lake Basins through Space and Time. AAPG Studies in Geology,* 46: 3–34.

Bottari, F., Marsili, A., Morelli, I. & Pacchiani, M., 1972. Aliphatic and triterpenoid hydrocarbons from ferns. *Phytochemistry,* 11: 2519–2523.

Brassell, S. C., Comet, P. A., Eglinton, G., Isaacson, P. J., McEvoy, J., Maxwell, J. R., Thompson, I. D., Tibbetts, P. J. C. & Volkman, J. K., 1980. The origin and fate of lipids in the Japan Trench. In: Douglas, A. G. & Maxwell, J. R. (eds.), *Advances in Organic Geochemistry 1979.* Pergamon Press, Oxford, pp. 375–392.

Bray, E. E. & Evans, E. D., 1961. Distribution of *n*-paraffins as a clue to the recognition of source beds. *Geochimica et Cosmochimica Acta*, 22: 2–15.

Budinova, T., Huang, W.-L., Racheva, I., Tsyntsarski, B., Petrova, B. & Yardim, M. F., 2014. Investigation of kerogen transformation during pyrolysis by applying a diamond anvil cell. *Oil Shale*, 31: 121–131.

Chaffee, A. L., Hoover, D. S., Johns, R. B. & Schweighard, F. K., 1986. Biological markers extractable from coal. In: Johns, R. B. (ed.), *Biological Markers in the Sedimentary Record*. Elsevier, Amsterdam, pp. 311–345.

Cranwell, P. A., Eglinton, G. & Robinson, N., 1987. Lipids of aquatic organisms as potential contributors to lacustrine sediments. *Organic Geochemistry*, 11: 513–527.

Dedić, Lj., 1978. Pojave magnezita u tercijarnom basenu Kremne. In: Čičić, S. (ed.), *Zbornik radova, IX Kongres geologa Jugoslavije, Sarajevo, 2–7 oktobar 1978. Publisher (izdavač), Organizacioni odbor IX kongresa geologa Jugoslavije, Sarajevo, October, 1978,* pp. 723–726. [In Serbian.]

Derenne, S., Largeau, C., Casadevall, E. & Connan, J., 1988. Comparison of torbanites of various origins and evolutionary stages. Bacterial contribution to their formation. Causes of the lack of botryococcane in bitumens. *Organic Geochemistry*, 12: 43–59.

Didyk, B. M., Simoneit, B. R. T., Brassell, S. C. & Eglinton, G., 1978. Organic geochemical indicators of paleoenvironmental conditions of sedimentation. *Nature*, 272: 216–222.

Dimitrijević, M. D. (ed.), 2000. *Geološki Atlas Srbije 1:2 000 000 (Br. 14). Metalogenetska karta i karta rudnih formacija*. Izdavač, Ministarstvo rudarstva i energetike Republike Srbije, Beograd. [In Serbian.]

Dragaš, M., Opić, I. & Britvić, V., 1991. Temperature distribution analysis in INA - Naftaplin's exploration provinces based on the temperature measurings. *Nafta*, 42: 383–398. [In Croatian, with English summary.]

Eremija, M., 1977. Kremanski basen. In: Petković, K. (ed.), *Geologija Srbije - II/3 - stratigrafija, kenozoik.* Zavod za regionalnu geologiju i paleontologiju, Belgrade, pp. 278–279. [In Serbian.]

Espitalié, J., Deroo, G. & Marquis, F., 1985. La pyrolyse Rock-Eval et ses applications. Première partie. *Revue de l'Institut Français du Pétrole*, 40: 563–579.

Floyd, P. A., Helvaci, C. & Mittwede, S. K., 1998. Geochemical discrimination of volcanic rocks associated with borate deposits: an exploration tool? *Journal of Geochemical Exploration,* 60: 185–205.

Golovko, A. K., 1997. *Neftyanie alkilaromaticheskie uglevodorodi*. Ph. D. Thesis, University of Tomsk, Russia, 352 pp. [In Russian.]

Grice, K., Schouten, S., Nissenbaum, A., Charrach, J. & Sinninghe Damsté, J., 1998a. Isotopically heavy carbon in the C_{21} to C_{25} regular isoprenoids in halite-rich deposits from the Sdom Formation, Dead Sea Basin, Israel. *Organic Geochemistry*, 28: 349–359.

Grice, K., Schouten, S., Peters, K. E. & Sinninghe Damsté, J., 1998b. Molecular isotopic characterization of hydrocarbon biomarkers in Palaeocene-Eocene evaporitic lacustrine source rocks from the Jianghan Basin, China. *Organic Geochemistry*, 29: 1745–1764.

Hughes, W. B., Holba, A. G. & Dzou, L. I. P., 1995. The ratios of dibenzothiophene to phenanthrene and pristane to phytane as indicators of depositional environment and lithology of petroleum source rocks. *Geochimica et Cosmochimica Acta*, 59: 3581–3598.

Huizinga, B. J., Aizenshtat, Z. A. & Peters K. E., 1988. Programmed pyrolysis-gas chromatography of artificially matured Green River kerogen. *Energy Fuels*, 2: 74–81.

Ilić, A. & Neubauer, F., 2005. Tertiary to recent oblique convergence and wrenching of the Central Dinarides: Constraints from a palaeostress study. *Tectonophysics*, 410: 465–484.

Ilić, M., 1969. Rezultati nekih novih istraživanja ležišta magnezita u okolini Raške. *Zbornik Radova Rudarsko-Geološkog Fakulteta,* 11/12: 89–127. [In Serbian.]

Ilić, M. M. & Rubežanin, D., 1978. O genezi magnezitskih ležišta zlatiborskog ultrabazitskog masiva. In: Čičić, S. (ed.), *Zbornik radova, IX Kongres geologa Jugoslavije, Sarajevo, 2–7 oktobar 1978. Publisher (izdavač), Organizacioni odbor IX kongresa geologa Jugoslavije, Sarajevo, October 1978*, pp. 539–554. [In Serbian.]

Ishiwatari, R. & Fukushima, K., 1979. Generation of unsaturated and aromatic hydrocarbons by thermal alteration of young kerogen. *Geochimica et Cosmochimica Acta*, 43: 1343–1349.

Jovančićević, B., Wehner, H., Scheeder, G., Stojanović, K., Šajnović, A., Cvetković, O., Ercegovac, M. & Vitorović, D., 2002. Search for source rocks of the crude oils of the Drmno depression (southern part of the Pannonian Basin, Serbia). *Journal of the Serbian Chemical Society*, 67: 553–566.

Kemp, P., Lander, D. J. & Orpin, C. G., 1984. The lipids of the rumen fungus Piromonas communis. *Journal of General Microbiology*, 130: 27–37.

Kleeman, G., Poralla, K., Englert, G., Kjosen, H., Liaaen-Jensen, N., Neunlist, S. & Rohmer, M., 1990. Tetrahymanol from the phototrophic bacterium Rhodopseudonomas palustris: First report of a gammacerane triterpane from a prokaryote. *Journal of General Microbiology*, 136: 2551–2553.

Kluska, B., Rospondek, M. J., Marynowski, L. & Schaeffer, P.,

2013. The Werra cyclotheme (Upper Permian, Fore-Sudetic Monocline, Poland): Insights into fluctuations of the sedimentary environment from organic geochemical studies. *Applied Geochemistry*, 29: 73–91.

Koopmans, M. P., de Leeuw, J. W. & Sinninghe Damsté, J. S., 1997. Novel cyclised and aromatised diagenetic products of β-carotene in the Green River Shale. *Organic Geochemistry*, 26: 451–466.

Koopmans, M. P., Köster, J., van Kaam-Peters, H. M. E., Kenig, F., Schouten, S., Hartgers, W. A., de Leeuw, J. W. & Sinninghe Damsté, J. S., 1996a. Diagenetic and catagenetic products of isorenieratene: Molecular indicators for photic zone anoxia. *Geochimica et Cosmochimica Acta*, 60: 4467–4496.

Koopmans, M. P., Schouten, S., Kohnen, M. E. L. & Sinninghe Damsté, J. S., 1996b. Restricted utility of aryl isoprenoids as indicators for photic anoxia. *Geochimica et Cosmochimica Acta*, 60: 4873-4876.

Kostić, A., 2010. *Thermal evolution of organic matter and petroleum generation modelling in the Pannonian Basin (Serbia)*. University of Belgrade, Faculty of Mining and Geology & "Planeta print", Belgrade, 150 pp. [In Serbian, with English summary.]

Kovačević, M., 1998. Sepiolite and Palygorskite Clay in Serbia. In: Šućur, M. (ed.), *Proceedings of the13th Congress of Yugoslav Geologists, Herceg Novi, October 6-9, 1998.* Published by the Geological Society of Montenegro, pp. 753–763. [In Serbian, with English summary.]

Krstić, N., Dumadžanov, N., Olujić, J., Vujanović, L. & Janković-Golubović, J., 2001. Interbedded tuff and bentonite in the Neogene lacustrine sediments of the central part of the Balkan Peninsula. A review. *Acta Vulcanologica*, 13: 91–99.

Lafargue, E., Marquis, F. & Pillot, D., 1998. Rock-Eval 6 applications in hydrocarbon exploration, production, and soil contamination studies. *Revue de l'Institut Français du Pétrole*, 53: 421–437.

Langford, F. F. & Blanc-Valleron, M. M., 1990. Interpreting Rock-Eval pyrolysis data using graphs of pyrolyzable hydrocarbons vs. total organic carbon. *American Association of Petroleum Geologists Bulletin*, 74: 799–804.

Mackie, A. V. E., Leng, J. M., Lloyd, M. J. & Arrowsmith, C., 2005. Bulk organic $\delta^{13}C$ and C/N ratios as palaeosalinity indicators within a Scottish isolation basin. *Journal of Quaternary Science*, 20: 303–312.

Maksimović, Z., 1996. Alteration of ultramafic rocks of Zlatibor. In: Dimitrijević, M. D. (ed.), *Geology of Zlatibor*. Geoinstitute Special Publication, 18: 39–40.

Marović, M., Djoković, I., Pešić, L., Radovanović, S., Toljić, M. & Gerzina, N., 2002. Neotectonics and seismicity of the southern margin of the Pannonian basin in Serbia. *EGU Stephan Mueller Special Publication Series*, 3: 277–295.

Marović, M., Krstić, N., Stanić, S., Cvetković, V. & Petrović, M., 1999. The evolution of Neogene sedimentation provinces of Central Balkan Peninsula. *Bulletin of Geoinstitute*, 36: 25–94. [In Serbian, with English summary.]

Meyers, P. A., 1994. Preservation of elemental and isotopic source identification of sedimentary organic matter. *Chemical Geology*, 114: 289–302.

Meyers, P. A., 1997. Organic geochemical proxies of paleoceanographic, paleolimnologic and paleoclimatic processes. *Organic Geochemistry*, 27: 213–250.

Meyers, P. A. & Ishiwatari, R., 1993. The early diagenesis of organic matter in lacustrine sediments. In: Engels, M. H. & Macko, S. A. (eds), *Organic Geochemistry: Principles and Applications.* Plenum Press, New York, pp. 185–209.

Mojsilović, S., Baklaić, D. & Đoković, I., 1973. *Basic Geological Map of SFRJ, Užice Sheet, Scale 1:100000*. Savezni geološki zavod, Beograd.

Moldowan, J. M., Seifert, W. K. & Gallegos, E. J., 1985. Relationship between petroleum composition and depositional environment of petroleum source rocks. *American Association of Petroleum Geologists Bulletin*, 69: 1255–1268.

Mrkić, S., Stojanović, K., Kostić, A., Nytoft, H. P. & Šajnović A., 2011. Organic geochemistry of Miocene source rocks from the Banat Depression (SE Pannonian Basin, Serbia). *Organic Geochemistry*, 42: 655–677.

Neto, E. V. D. S., Hayes, J. M. & Takaki, T., 1998. Isotopic biogeochemistry of the Neocomian lacustrine and Upper Aptian marine-evaporitic sediments of the Potiguar Basin, Northeastern Brazil. *Organic Geochemistry*, 28: 361–381.

Neunlist, S. & Rohmer, M., 1985. Novel hopanoids from the methylotrophic bacteria *Methylococcus capsulatus* and *Methylomonas methanica*. (22S)-35-aminobacteriohopane-30,31,32,33,34-pentol and (22S)-35-amino-3β-methylbacteriohopane-30,31,32,33,34-pentol. *Biochemical Journal*, 231**:** 635–639.

Obradović, J., Đurđević-Colson, J., Vasić, N., Radaković, A., Grubin, N. & Potkonjak, B., 1994. Carbonates from Neogene lacustrine basins of Serbia – geochemical characteristics. *Annales Géologiques de la Péninsule Balkanique*, 56: 177–199. [In Serbian, with English summary.]

Obradović, J., Nosin, V., Vasić, N. & Grubin, N., 1995. Contribution to the knowledge of the isotopic composition of carbonates from lacustrine basins of Serbia. *Collection of papers of the Faculty of Mining and Geology*, 57: 3–11. [In Serbian, with English summary.]

Obradović, J. & Vasić, N., 2007. *Jezerski baseni u Neogenu Srbije*. Srpska Akademija nauka i umetnosti, posebna izdanja, Odeljenje za matematiku, fiziku i geo-nauke, Knjiga 3, Belgrade, 310 pp. [In Serbian.]

Obradović, J., Vasić, N., Đorđević-Colson, J. & Grubin, N., 1996. Tertiary lacustrine basins of the Zlatibor complex. In: Dimitrijević, M. D. (ed.), *Geology of Zlatibor, Geoinstitute Special Publication, Belgrade*, 18: 97–104.

Ourisson, G., Albrecht, P. & Rohmer, M., 1979. The hopanoids: palaeo-chemistry and biochemistry of a group of natural products. *Pure and Applied Chemistry*, 51: 709–729.

Pantić, N., 1956. Biostratigrafija tercijarne flore Srbije. *Annales Géologiques de la Péninsule Balkanique*, 24: 199–321. [In Serbian.]

Parsi, Z., Hartog, N., Górecki, T. & Poerschmann, J., 2007. Analytical pyrolysis as a tool for the characterization of natural organic matter – A comparison of different approaches**.** *Journal of Analytical and Applied Pyrolysis*, 79: 9–15.

Peters, K. E., Walters, C. C. & Moldowan, J. M., 2005. *The Biomarker Guide, Volume 2: Biomarkers and Isotopes in the Petroleum Exploration and Earth History*. Cambridge University Press, Cambridge, 475–1155 pp.

Philp, R. P., 1985. *Fossil Fuel Biomarkers: Applications and Spectra*. *Methods in Geochemistry and Geophysics*. Elsevier, Amsterdam, 294 pp.

Platt, N. H. & Wright, V. P., 1991. Lacustrine carbonates: facies models, facies distributions and hydrocarbon aspects. In: Anadón, P., Cabrera, L. & Kelts, K (eds), *Lacustrine Facies Analysis.* International Association of Sedimentologists Special Publication, 13: 57–74.

Prysjazhnjuk, V., Kovalenko, V. & Krstić, N., 2000. On the terrestrial and freshwater mollusks from Neogene of Western Serbia. In: Karamata, S. & Janković, S. (eds), *Geology and Metallogeny of the Dinarides and the Vardar zone*. Academy of Sciences and Arts of the Republic of Srpska, Banja Luka,

pp. 219-224. [In Serbian, with English summary.]

Radke, M., 1987. *Organic geochemistry of aromatic hydrocarbons*. In: Radke, M. (ed.), *Advances in Petroleum Geochemistry*. Academic Press, London, pp.141–205.

Radke, M. & Welte, D. H., 1983. The methylphenanthrene index (MPI): a maturity parameter based on aromatic hydrocarbons. In: Bjorřy, M., Albrecht, P., Cornford, C., de Groot, K., Eglinton, G., Galimov, E., Leythaeuser, D., Pelet, R., Rullkötter, J. & Speers, G. (eds), *Advances in Organic Geochemistry 1981.* John Wiley & Sons Limited, Chichester, pp. 504–512.

Radke, M., Welte, D. H. & Willsch, H., 1982a. Geochemical study on a well in the Western Canada Basin: relation of the aromatic distribution pattern to maturity of organic matter. *Geochimica et Cosmochimica Acta*, 46: 1–10.

Radke, M., Willsch, H., Leythaeuser, D. & Teichmüller, M., 1982b. Aromatic components of coal: relation of distribution pattern to rank. *Geochimica et Cosmochimica Acta*, 46: 1831–1848.

Risatti, J. B., Rowland, S. J., Yon, D. A. & Maxwell, J. R., 1984. Stereochemical studies of acyclic isoprenoids- XII. Lipids of methanogenic bacteria and possible contributions to sediments. *Organic Geochemistry*, 6: 93–103.

Rohmer, M., Bisseret, P. & Neunlist, S., 1992. The hopanoids, prokaryotic triterpenoids and precursors of ubiquitous molecular fossils. In: Moldowan, J. M., Albrecht, P. & Philp, R. P. (eds), *Biological Markers in Sediments and Petroleum*. Prentice Hall, Englewood Cliffs, NJ, pp. 1–17.

Schouten, S., Van der Maarel, M. J. E. C., Huber, R. & Sinninghe Damsté, J. S., 1997. 2,6,10,15,19-Pentamethylicosenes in *Methanolobus bombayensis*, a marine methanogenic archaeon, and in *Methanosarcina mazei. Organic Geochemistry*, 26: 409–414.

Schwark, L., Vliex, M. & Schaeffer, P., 1998. Geochemical characterization of Malm Zeta laminated carbonates from the Franconian Alb, SW-Germany (II). *Organic Geochemistry*, 29: 1921–1952.

Shanmugam, G., 1985. Significance of coniferous rain forests and related oil, Gippsland Basin, Australia. *American Association of Petroleum Geologists Bulletin*, 69: 1241–1254.

Sheppard, R. & Gude, A., 1973. Boron-bearing potassium feldspar of authigenic origin closed-basin deposits. *U.S. Geological Survey Journal of Research*, 1: 377–382.

Sinninghe Damsté, J. S., Keely, B. J., Betts, S. E., Baas, M., Maxwell, J. R. & de Leeuw, J. W., 1993. Variations in abundances and distributions of isoprenoid chromans and long-chain alkylbenzenes in sediments of the Mulhouse Basin: a molecular sedimentary record of palaeosalinity. *Organic Geochemistry*, 20: 1201–1215.

Sinninghe Damsté, J. S., Kenig, F., Koopmans, M. P., Köster, J., Schouten, S., Hayes, J. M. & de Leeuw, J. W., 1995. Evidence for gammacerane as an indicator of water column stratification. *Geochimica et Cosmochimica Acta*, 59: 1895–1900.

Sinninghe Damsté, J. S., Kock-Van Dalen, A. C., de Leeuw, J. W., Schenck, P. A., Guoying, S. & Brassell, S. C., 1987. The identification of mono-, di-and tri-methyl 2-methyl-2-(4,8,12-trimethyltridecyl)chromans and their occurrence in the geosphere. *Geochimica et Cosmochimica Acta*, 51: 2393–2400.

Sinninghe Damsté, J. S., Rijpstra, I., de Leeuw, J. W. & Schenck, P. A., 1989. The occurrence and identification of series of organic sulfur compounds in oils and sediment extracts. II. Their presence in samples from hypersaline and non-hypersaline palaeoenvironmental and maturity indicators. *Geochimica et Cosmochimica Acta*, 53: 1323–1341.

Stamatakis, M. G., 1989. A boron-bearign potassium feldspar in volcanic ash and tuffaceous rocks from Miocene lake deposits, Samos Island, Greece. *American Mineralogist*, 74: 230–235.

Stojanović, K., Jovančićević, B., Šajnović, A., Sabo, T., Vitorović, D., Schwarzbauer, J. & Golovko, A., 2009. Pyrolysis and Pt(IV)- and Ru(III)-ion catalyzed pyrolysis of asphaltenes in organic geochemical investigation of a biodegraded crude oil (Gaj, Serbia). *Fuel*, 88: 287–296.

Stojanović, K., Jovančićević, B., Vitorović, D., Pevneva, G., Golovko, J. & Golovko, A., 2007. New maturation parameters based on naphthalene and phenanthrene isomerization and dealkylation processes aimed at improved classification of crude oils (Southeastern Pannonian Basin, Serbia). *Geochemistry International*, 45: 781–797.

Stojanović, K., Šajnović, A., Sabo, T., Golovko, A. & Jovančićević, B., 2010. Pyrolysis and Catalyzed Pyrolysis in the Investigation of a Neogene Shale Potential from Valjevo-Mionica Basin, Serbia. *Energy & Fuel*, 24: 4357–4368.

Suggate, R. P., 1998. Relations between depth of burial, vitrinite reflectance and geothermal gradient. *Journal of Petroleum Geology*, 21: 5–32.

Szabó, Cs., Molnár, F. & Kiss, G., 2009. Mineralogy and origin of the Piskanja borate deposit (Jarandol basin, Serbia). *Mitteilungen der Österreichischen Mineralogischen Gesellschaft*, 155: 153.

Šajnović, A., Simić, V., Jovančićević, B., Cvetković, O., Dimitrijević, R. & Grubin N., 2008a. Sedimentation History of Neogene Lacustrine Sediments of Sušeočka Bela Stena Based on Geochemical Parameters (Valjevo-Mionica Basin, Serbia). *Acta Geologica Sinica – English Edition*, 82: 1201–1212.

Šajnović, A., Stojanović, K., Jovančićević, B. & Cvetković, O., 2008b. Biomarker distributions as indicators for the depositional environment of lacustrine sediments in the Valjevo-Mionica basin (Serbia). *Chemie der Erde – Geochemistry*, 68: 395–411.

Šajnović, A., Stojanović, K., Jovančićević, B. & Golovko, A., 2009. Geochemical investigation and characterisation of Neogene sediments from Valjevo-Mionica Basin (Serbia). *Environmental Geology*, 56: 1629–1641.

Šajnović, A., Stojanović, K., Simić, V. & Jovančićević, B., 2012. Geochemical and Sedimentation History of Neogene Lacustrine Sediments from the Valjevo-Mionica Basin (Serbia). In: Panagiotaras, D. (ed.), *Geochemistry – Earth's System Processes*. InTech, Rijeka, pp. 1–26.

ten Haven, H. L., de Leeuw, J. W., Rullkötter, J. & Sinninghe Damsté, J. S., 1987. Restricted utility of the pristane/phytane ratio as a palaeoenvironmental indicator. *Nature,* 330: 641–643.

Tucker, M. E. & Wright, V. P. 1990. *Carbonate Sedimentology*. 482 pp. Blackwell Scientific Publications, Oxford.

Utescher, T., Djordjevic-Milutinovic, D., Bruch, A. & Mosbrugger, V., 2007. Palaeoclimate and vegetation change in Serbia during the last 30 Ma. *Palaeogeography, Palaeoclimatology Palaeoecology*, 253: 141–152.

van Aarssen, B. G. K., Bastow, T. P., Alexander, R. & Kagi, R. I., 1999. Distributions of methylated naphthalenes in crude oils: indicators of maturity, biodegradation and mixing. *Organic Geochemistry*, 30: 1213–1227.

Vink, A., Schouten, S., Sephton, S. & Sinninghe Damsté, J. S., 1998. A newly discovered norisoprenoid, 2,6,15,19-tetramethylicosane, in Cretaceous black shales. *Geochimica et Cosmochimica Acta*, 62: 965–970.

Volkman, J. K., 1986. A review of sterol markers for marine and

terrigenous organic matter. *Organic Geochemistry,* 9: 83–99.

Volkman, J. K., 2003. Sterols in microorganisms. *Applied Microbiology and Biotechnology*, 60: 496–506.

Volkman, J. K., Allen, D. I., Stevenson, P. L. & Burton, H. R., 1986. Bacterial and algal hydrocarbons from a saline Antarctic lake, Ace Lake. *Organic Geochemistry*, 10: 671–681.

Wang, R. & Fu, J., 1997. Variability in biomarkers of different saline basins in China. *International Journal of Salt Lake Research (Hydrobiologia)*, 6: 25–53.

Waples, D. W., Haug, P. & Welte, D. H., 1974. Occurrence of a regular C_{25} isoprenoid hydrocarbon i Tertiary sediments representing a lagoonal-type, saline environment. *Geochimica et Cosmochimica Acta,* 62: 381–387.

Wolff, G. A., Ruskin, N. & Marshal, J. D., 1992. Biogeochemistry of an early diagenetic concretion from the Birchi Bed (L. Lias, W. Dorset, UK). *Organic Geochemistry*, 19: 431–444.

Yangming, Z., Huanxin, W., Aiguo, S., Digang, L. & Dehua, P., 2005. Geochemical characteristics of Tertiary saline lacustrine oils in the Western Qaidam Basin, northwest China. *Applied Geochemistry*, 20: 1875–1889.

Yawanarajah, S. R. & Kruge, M. A., 1994. Lacustrine shales and oil shales from Stellarton Basin, Nova Scotia, Canada: organofacies variations and use of polyaromatic hydrocarbons as maturity indicators. *Organic Geochemistry*, 21: 153–170.

Yoshioka, H. & Ishiwatari, R., 2002. Characterization of organic matter generated from Green River shale by infrared laser pyrolysis. *Geochemical Journal*, 36: 73–82.

Zander, J. M., Caspi, E., Pandey, G. N. & Mitra, C. R., 1969. The presence of tetrahymanol in Oleandra wallichii. *Phytochemistry*, 8: 2265–2267.

Živković, M. & Stojanović, D., 1976. Sirlezit u sedimentnom magnezitu Kremne kod Titovog Užica. *Vatrostalni materijali*, 6: 3–8. [In Serbian.]